Title

THE STRENGTH AND DUCTILITY OF METASTAELE AUSTENITIC STEELS AS A FUNCTION OF COMPOSITION AND TEST TEMPERATURES.

Author

Chanani, Govind Ram

Publication Date

1967-09-01

UCRL-17805

C.2

University of California

Ernest O. Lawrence Radiation Laboratory

THE STRENGTH AND DUCTILITY
OF METASTABLE AUSTENITIC STEELS
AS A FUNCTION OF COMPOSITION
AND TEST TEMPERATURES

Govind Ram Chanani
(M. S. Thesis)

September 1967

DISCLAIMER

UCRL-17805

UNIVERSITY OF CALIFORNIA

Lawrence Radiation Laboratory
Berkeley, California

AEC Contract No. W-7405-eng-48

THE STRENGTH AND DUCTILITY OF METASTABLE AUSTENITIC STEELS AS A FUNCTION OF COMPOSITION AND TEST TEMPERATURES

Govind Ram Chanani

(M.S. Thesis)

September 1967

TABLE OF CONTENTS

THE STRENGTH AND DUCTILITY OF METASTABLE AUSTENITIC STEELS AS A FUNCTION OF COMPOSITION AND TEST TEMPERATURES

Govind Ram Chanani

Inorganic Materials Research Division, Lawrence Radiation Laboratory, Department of Mineral Technology, College of Engineering, of the University of California, Berkeley, California

ABSTRACT

The present investigation was made to study the combined and individual effects of composition, test temperature and temperature of deformation on the tensile properties and strain-hardening characteristics of metastable austenitic steels. The results obtained indicate unusual combinations of strength and ductility for the steels in a certain carbon range after suitable thermomechanical processing.

The strength and ductility were retained in the temperature range of -196°C to 100°C. However, when tested at 200°C, which is above M_D, the material exhibited lower ductility.

A CDC 6600 computer (Fortran IV) was used to determine the true stress-true strain relationship and strain hardening exponent.

In the present investigation, certain thermo-mechanical treatments produced steels having yield strengths in the range of 200,000 to 300,000 psi with 30 to 20% elongation, respectively. The improved ductility for these steels compared to conventional high strength steels is attributed to the martensitic transformation occurring during testing which is thought to inhibit incipient necking.

1. INTRODUCTION

Yield and tensile strengths and ductility are the commonly measured mechanical properties of a metal or alloy as these are of immense value. For any engineering material, it is always desirable to have high strength and high ductility. Various strengthening mechanisms have been devised, but their usefulness is limited due to associated low value of ductility. In general, there exists an inverse relationship between strength and ductility; for example, when cold working is done to increase the strength, ductility is lost. However, thermomechanical processes have been developed for certain ferrous alloys which result in a good balance of strength and ductility.

A conventional and common method of strengthening is cold working. The dislocations introduced in the material during cold working are arranged in a cell structure, i.e. here tangles of dislocations are formed.[1,2] The strength of the material depends on the cell size since the walls of the cells act as barriers to the motion of the slip dislocations. The smaller the distance between the cell walls i.e. smaller the cell size, the higher is the strength. But as the cell size is decreased, ductility is lost because the motion of dislocations is impeded.

Precipitation hardening is another common method of strengthening. Here the precipitates resist the dislocation motion by pinning. Ductility is lost because of the lower strain hardening rate. The maximum ductility obtainable is in the range of 10-15%.

Maraging steels possess a good combination of strength and ductility.[3] Here the strengthening is attributed to the presence of a finely dispersed precipitate. Plastic straining of the austenite prior to the phase

transformation in the case of these alloys gives only slightly improved properties.[3]

The most promising among the various thermo-mechanical processes developed to date is "ausforming". In this process, metastable austenite is deformed prior to transformation to martensite. Usually this is applicable in case of an alloy system which exhibits a "bay" region in the T-T-T diagram where the deformation can be suitably carried out. Strengthening is attributed mainly to two factors:

1. high dislocation density produced,
2. the dispersion of alloy carbides formed during the deformation of austenite.

The first is believed to be more important.[4]

Further improvement in the properties can be obtained by dynamic strain aging.[5] In this process straining is done at an elevated temperature where aging may occur simultaneously.

In the present investigation, thermomechanical treatments, devised for certain metastable austenitic steels, have been found to result in unusual combinations of strength and ductility. The ductility during tensile testing is believed to be due to the transformation induced plasticity (a phenomenon known as TRIP).[14] In this case, metastable austenite transforms to martensite during testing.

The formation of martensite during tensile testing increases strain hardening since it is a harder phase than the parent austenite. This higher strain hardening rate inhibits local necking, i.e., plastic instability, and thereby higher ductility is obtained. The transformation of austenite to martesnite in case of various austenitic stainless steels

has been studied extensively as a function of plastic strain[6-9] and temperature of deformation.[8,10-13] At a temperature below M_D temperature (M_D is the temperature above which no martensite can be obtained by plastic deformation), there is a critical strain beyond which the parent austenite undergoes martensitic transformation. This strain is first exceeded at the point of plastic instability (i.e., local necking), as a result martensite forms and necking is inhibited.

During the tensile tests of 301 and 304 steels,[15] Bressanelli and Moskowitz have also found a similar beneficial effect of martensite formation on the tensile elongation. They reported that a specific amount of martensite formation is most beneficial. According to them only the martensite formed in the later stages of tensile testing, i.e. during necking, is beneficial. Composition and test temperatures directly affect the amount of martensite formed during testing and hence the elongation and strength.

The present investigation was planned to carry out further work on TRIP phenomena in order to find 1) the dependence of TRIP on composition with particular emphasis on the effect of carbon content since carbon has a significant effect on M_S temperature (temperature below which martensitic transformation takes place on cooling), on M_D temperature, and on the total amount of martensite formed during testing. As a result, the amount of carbon has an important bearing on strength as well as on ductility because the transformation characteristics control local necking and hence elongation; 2) effect of processing temperature on TRIP - the processing temperature is also a very important variable. If this is below the M_D temperature, austenite will transform to martensite and

hence during tensile testing the TRIP phenomenon cannot be operative. A very high processing temperature enhances diffusion resulting recovery and coarsening of precipitates with consequent loss in strength; 3) mechanical properties (i.e. $\sigma_{Y.S.}$, $\sigma_{U.T.S.}$ and % elongation) of TRIP steels at different test temperatures (-196°C to 200°C). Since the transformation is strongly temperature dependent, the temperature of testing will have a significant effect on the mechanical properties. At a lower temperature of testing, the critical strain for the start of transformation should be smaller because the chemical driving force for the transformation is higher. Above M_D, no TRIP phenomenon will occur; 4) strain hardening characteristics of these steels as a function of temperature of testing (-196°C to 200°C) and carbon content (0.05-0.5% carbon). The strain hardening rate has direct bearing on the onset of necking.[16] Since strain hardening is obviously effected by the martensite formation during testing, it is useful to correlate the effects of processing temperatures, test temperatures and carbon content on transformation with strain hardening characteristics of steels.

2. EXPERIMENTAL PROCEDURE

2.1 Selection of Alloys

The alloys used for the investigation were selected on the basis of previous work with high strength metastable austenitic steels.[14,18,19]

A suitable balance of various alloying elements and carbon was made so that the metastable austenitic steels have M_S temperatures well below room temperature, while the M_D temperature is above room temperature after the thermomechanical processing. The austenite is designed to have a high work hardening rate, high stability and extensive precipitation hardening with deformation at a suitable elevated temperature. Carbon was the main variable. Alloys with carbon from 0.05 to 0.5% were tested. The compositions used are shown in Table I.

The composition of alloys a to i is similar to that of j to m except for Cr content which is in the range of 8.5% to 9.5% in the former alloys and approximately 12% in the later alloys. All the alloys have Mo content of about 4% except for a and f which have approximately 1% Mo. All these alloys have been studied with respect to the various processing temperatures and temperatures of testing.

2.2 Alloy Processing

The steels to be used were prepared by induction melting of high purity elements under vacuum. The ingots were hot forged at 1100°C to 2-1/2 in. ×1/4 in. The bar stock was then cleaned of surface scale prior to the subsequent heat treatment.

The bars were then austenitized at 1100°C for one hour under an atmosphere of 4% hydrogen in helium (forming gas) and then water quenched.

The material was then deformed 80% at various temperatures. Deformation

temperatures of 550°C, 450°C, 350°C, 250°C and room temperature were selected on the basis of previous work.[14,18,19] Deformation was carried out by means of heated rolls.

The material was reheated in an electric furnace between passes. The whole process of reducing the thickness from 0.25 in. to 0.05 in. (80% reduction) required less than one hour. After rolling the material was water quenched.

2.3 Mechanical Testing

Tensile specimens were prepared and tested at various temperatures on an Instron testing machine using a crosshead speed of 0.1 cms/min. The dimensions of the tensile specimens are shown in Fig. 1.

To perform isothermal tests at various temperatures and to absorb the heat of deformation involved, the specimens were surrounded by a cylindrical container. The container was filled with liquid nitrogen for the tests at -196°C. For tests at 100°C boiling distilled water heated by an immersion coil heater was used. Oil was heated by an immersion heater for the tests at 200°C. Occasional stirring of the bath maintained a constant temperature.

2.4 Determination of Strain Hardening Characteristics

To study the strain hardening characteristics, it was necessary to derive the true stress-true strain relationship for the various tensile tests in order to find the value of strain hardening exponent.

Due to the large number of specimens tested, a CDC 6600 computer (Fortran IV) was used to compute the values of true stress and true strain directly from the load extension curves obtained by Instron.

The strain hardening exponent (n) is related to the true stress (σ) and the true strain (ϵ) in the following manner

$$\sigma = A\epsilon^{n}$$

where A is a constant known as strength coefficient. By solving for n and differentiating

$$n = \frac{d\ (\log \sigma)}{d\ (\log \epsilon)}$$

it is obvious that the strain hardening exponent is given by the slope of a log-log plot of true stress versus true strain. For this purpose, only that portion of the load extension curve was used which showed strain hardening and no necking (i.e. only past the Lüders' strain and before the maximum load).

A least squares polynominal fit was made to obtain the slope of the log-log plot, i.e., the value of the strain hardening exponent.

2.5 Estimation of the Amount of Martensitic Transformation

The transformation was qualitatively observed by means of a strong hand magnet. It was assumed that the specimens which were non-magnetic were austenitic and that those which were strongly magnetic were martensitic. Those specimens showing intermediate response to the magnet were assumed to have undergone only partialy transformation to martensite.

3. RESULTS AND DISCUSSION

3.1 General

The properties of the alloys in the annealed condition are shown in Table II. Tables III through XV show the properties of the alloys at various test temperatures after various kinds of processing. It can be seen that the alloys with carbon content in the range of 0.2-0.3% exhibit yield strengths above 200,000 psi with an elongation of 20-30% after 80% deformation above M_D. The improved mechanical properties are the result of changes occurring during thermomechanical processing as well as those during testing. The higher strength of these alloys, compared to the annealed material, can be attributed to those same mechanisms operative in the case of ausformed steels since there is a similarity in processing. The tensile elongation and other properties can be discussed on the basis of the transformation which the metastable austenitic alloys undergo during straining. In the case of high strength steels, it is believed that plastic instability (the onset of necking) is responsible for low values of elongation. It has been observed in many cases[22] that although the reduction in area is high (implying a high value of local elongation) the total elongation is considerably lower. Hence, if necking could be prevented, the elongation would be enhanced.

The criteria for the onset of necking is[16]

$$\frac{d\sigma}{d\epsilon} = \sigma = n$$

where σ, ϵ, and n are true stress, true strain and strain hardening exponents, respectively. This means if the value of flow stress is

increased, the rate of strain hardening must also be increased to avoid or to delay necking. In conventional high strength steels, strain hardening is due to dislocation interactions and the effectiveness of these appears to decrease as the strength is increased. As a result uniform elongation decreases. It appears that the strain induced transformation of austenite to martensite provides strong barriers which enhance the strain hardening rate. The exact nature of these barriers is not yet known. It can be assumed that since martensite is a phase harder and stronger then the parent austenite it provides a stronger barrier than the work-hardened austenite. At the same time due to the higher volume of martensite and the inherent spontaneous nature of transformation a very high dislocation density is probably produced.

The fact that the transformation of austenite to martensite during testing gives higher elongation has been reported by various investigators.[14,15,20] The improved tensile elongation for 301 and 304 steels obtained by Bressanelli and Moskowitz has been mentioned earlier.

In conclusion, deformation of austenite above room temperature but below the recrystallization temperature results in significant changes in both the structure and the composition of the austenite. In alloy steels, alloy carbides precipitate on extremely fine scales during the deformation. The precipitation results in a depletion of carbon in the matrix and thus causes an elevation of the M_S and M_D temperatures. The steels used in the present investigation are austenitic in general after thermomechanical processing (except for those deformed at 25°C) and have a high dislocation density and a fine dispersion of alloy carbides. In addition, the alloys transform to martensite during testing, thus giving enhanced ductility.

In this report the effect of process variables on the properties are discussed with respect to the martensitic transformation.

3.2 Effect of Processing and Testing Temperature Shape of Load-Extension Curves

A large number of load-extension curves were obtained for different specimens, but, as many of these were similar in form, they are not all presented in this report. Instead, the types of load-extension curves encountered are shown schematically in Fig. 2.

It can be seen from Table II for the the fully annealed alloys, the curves are mostly of two major types, i.e., type I or IA at testing temperatures below room temperature (22°C) and type VII or VIIA at room temperature and above. At lower testing temperature, the curves show more work hardening because of the increased amount of martensitic transformation. Except for the slopes, type I and VII curves are typical of austenitic steels.

When the alloys were deformed 80% at 25°C, the curves fell in the category of type II, IIA or III. These curves are characteristic of a brittle material. Magnetic response shows that these specimens were strongly magnetic before testing which implies that these are martensitic and hence high elongation is not expected.

In the case of those specimens processed 80% at 250°C, 350°C, 450°C, and 550°C, the temperature of testing plays a significant effect on the nature of curves as can be seen in Tables V-VIII. The amount of carbon also has some effect. The effect of carbon is more pronounced in the higher carbon range as shown in Tables VII and VIII.

At -196°C (liquid nitrogen testing), the curves are mostly of type IV,

with some belonging to the type V. In these cases, a very steep rise in the curve follows a considerable amount of Lüders' type strain. These specimens also show a marked yield point. The Lüders' strain region is serrated which may be associated with martensitic transformation (to be discussed later).

At -78°C and 22°C, type VI or VIA are mostly observed. These are similar to the type IV except that the Lüders' bands are not so pronounced and that the slope of the curve past the band is lower and some of the specimens which have carbon in the vicinity of 0.3% (e.g. alloy i) and have been deformed at 450°C show type VIII or VIIIA. Also the higher carbon (0.4 and 0.5) specimens, when deformed 20%, exhibit load extension curves of type VIIIA (Table XIV). These are highly serrated and most of the strain is by Lüders' band propogation. These specimens show higher ductility than the others.

Specimens tested at 100°C follow in general the load extension path of type X except for the specimens of alloy j (0.05°C) deformed 80% at 450°C and 550°C, which in contrast follow type IX. The type X curves are serrated for the entire range and exhibit a higher value of total elongation. Here the transformation is most favorable in the sense that it appears to take place at the appropriate value of strain to inhibit necking. Alloy j, because of its low carbon (0.05%) has the highest M_D. Subsequently it transforms to martensite very easily and probably at a very low value of strain and as a result necking is not inhibited.

Total elongation is decreased resulting in a curve of type IX. The serrations observed at 100°C are typical of metastable steels.[15,21] Here the sudden decrease in load after some strain is due to the localized

necking of the specimen, and the sudden recovery in the load is attributed to the formation of martensite in the necking region.

At 200°C, which is above M_D, the curves of type II are invariably obtained. As mentioned earlier, these curves are typical of brittle materials. Since 200°C is above M_D, no transformation takes place and as a result local necking is not inhibited. Magnetic response shows that the specimens have the same amount of martensite before after testing.

3.3 Effect of Testing Temperatures on the Properties

It is obvious from the Tables II to VIII that the alloys studied show a wide range of properties at different test temperatures. The strength for a particular alloy after processing may vary as much as 50% depending on the test temperature while the elongation may vary from 1 to 40%. The strain hardening exponent (n) also varies from very near zero to as high as unity.

3.3.1 Effect of Testing Temperature on the Strength and Ductility of the Steels

As can be seen from the Fig. 3, the annealed alloys, which are completely austenitic before testing, show a decrease in strength and an increase in elongation with increase in temperature of testing. The alloys were designed in such a way that their M_S temperatures were well below room temperature and their M_D temperatures much higher than room temperature. The continuous drop in strength with rise in testing temperature as shown in Fig. 3 is typical of conventional steels. The elongation also increases with temperature as expected except above 100°C. In these steels, the TRIP phenomenon is operative and the drop in elongation can be explained on the basis of this. At -196°C both the lower carbon alloys which are

partially martensitic initially, and the higher carbon alloys which are completely austenitic, probably transform to martensite during the early stage of straining. It is thought that the martensite so produced is not as beneficial to elongation.

The rate of transformation for the annealed alloys is optimum at 22°C and 100°C. At 200°C, the amount of transformation is very small as can be seen by the magnetic response, i.e., the alloys l and m are completely austenitic after testing while the alloys j and k are mostly austenitic. Due to the lack of transformation, ductility was small at 200°C.

The strength and ductility of various alloys after processing as a function of test temperatures are shown in Figs. 4 to 7.

In general the yield strength is maximum at -196°C and decreases with increasing temperature of testing up to 22°C testing. The strength then increased with increasing temperature above 22°C. The higher value of yield strength at lower temperature is expected. The elongation is nearly constant in the range of -196°C to 22°C, but shows an increase at 100°C. The elongation drops to a very low value at 200°C. At this temperature, the specimens do not show any significant change in their magnetic response after testing which indicates that the transformation does not take place.

These results are in agreement with those obtained by Bressanelli and Moskowitz[15] who also obtained a peak in elongation vs testing temperature and concluded that the formation of either greater or lesser amounts of martensite than a specific amount results in less than optimum elongation. In the present case, it can be assumed that an optimum amount of martensite is formed at 100°C.

3.3.2 Effect of Testing Temperature on Strain-Hardening Characteristics of TRIP steels.

The influence of testing temperature on the strain-hardening characteristic of austenitic steels has been studied by G. W. Powell, et al.[23] in detail. According to their work the strain-hardening characteristics of austenitic stainless steels are strongly dependent upon the stability of austenite. The present investigation shows a similar dependence.

Figure 10 shows the change in strain-hardening exponent, n, for fully annealed alloys as a function of the testing temperature. Figures 20 (a) and 21 (a,b) show true stress-true strain curves for alloy k at various temperatures as plotted by the computer. The true stress-true strain curves for other annealed alloys are similar in shape.

As seen in Fig. 21 (b), the annealed alloy shows a parabolic curve at 100°C, when a negligible amount of martensite is formed. This parabolic curve is characteristic of stable austenite. At lower temperatures, when the transformation takes place during testing, a departure from parabolic curves is observed. In these cases, the curves are quite steep in the initial stage but start flattening at higher strain. This effect is very pronounced in Fig. 20 (a). In this case martensite is formed at a very low value of strain due to the lower temperature of testing (-196°C). This is reflected in the strong magnetic response of a specimen strained only 4% at -196°C. This martensite plus the auto catalytic nature of the martensitic transformation gives rise to the initial stimulating effect. The value of strain hardening exponent, n, goes down somewhat with the rise in testing temperature as seen from Fig. 10.

The stress-strain relationships for the processed alloys show a large deviation from those of the annealed alloys.

Figures 22 and 23 show the true stress-true strain curves as well as log-log plots of the true stress-true strain relationships tested at four different temperatures for alloy k after 80% deformation at 350°C. Figures 11-14 indicate the variation of strain hardening exponent, n, with testing temperature for different alloys after processing at various temperatures. The strain hardening exponent, n, decreases linearly with increase in test temperature. This change in n with temperature is much larger in the case of processed alloys than for annealed alloys because of the lower stability of the processed alloys. The dependence of elongation on the value of n is shown in Fig. 24. The fact that the strain hardening rate is higher at -196°C suggests that the elongation should also be greater at this temperature. But as has been discussed earlier, this is not true in this case because of the formation of a greater amount of martensite at lower temperatures. If the austenitic steels could be extended in tension at lower temperatures without the formation of an excessive amount of martensite, the total elongation should increase. It can be seen in Fig. 22(a) for the specimen tested at -196°C that during the earlier stage, the curve does not show any upward trend. In this strain region, the deformation proceeds by Lüders' band propagation. Figure 23 (a) also shows a similar trend for the specimen tested at 22°C, but the range of strain spanned by band propagation is smaller than for the case of the specimen tested at -196°C. Here the band motion would be observed by the naked eye. The bands were seen to proceed from one grip end of specimen to the other, until the whole of specimen has been transformed. After this the load began to increase as seen in the later part of the curves in Figs. 22 (a) and 23 (a).

At 100°C, the upward rise in the curve is gradual and uniform for the entire region. Here the specimen strains by a Lüders' band propagation for the entire elongation. Also the martensitic formation is delayed until the later stage, thereby giving a higher elongation.[15]

In effect, the strain hardening characteristics are strongly dependent on the stability of austenite and the effect that temperature has on that stability.

3.4 Effect of Composition on Properties

As discussed in the introduction, chemical composition is one of the main factors governing the characteristics of martensitic transformation in any alloy. In the present investigation, the effect of carbon has been studied in detail as it is well known that carbon has a significant effect on both the M_S and M_D temperatures as well as on the strengths and ductility of the steels. Alloys with two different molybdenum content were also investigated.

As seen from Tables VII and VIII, yield strength varies from 130 to 245,000 psi while elongation varies from 30 to 0 percent, (depending on the carbon content) for the same treatment and same temperature of testing for otherwise similar alloys. At room temperature, the strain hardening exponent also varies from 0.30 to 0.60 with the carbon content only.

3.4.1 Effect of composition on the strength and ductility of the steels.

The variation of strength and ductility at 22°C and -196°C with % carbon is shown in Figs. 8 and 9. Since the properties do not follow a general pattern, they are enclosed by bands. In general, the strength rises with increase in carbon which is indicated by the upward slope of

the band. Alloy j with 0.05 carbon, when deformed 80% at 450°C and 550°C, shows behavior different from that of the others. Its strength is higher than the alloys with greater amount of carbon. As can be seen from Tables VII and VIII, this alloy is magnetic before testing which implies that it is somewhat martensitic and naturally its yield strength is higher than the others which are austenitic (non-magnetic) before testing. By statistical methods, Angel[17] obtained the following multiple regression equation for M_D.

$$M_{D\ 30}\,^{\circ}C = 413 - 462\,[(C+N)] - 9.2\,[Si] - 8.1\,[Mn] - 13.7\,[Cr] - 9.5\,[Ni] - 18.5\,[Mo]\ ,$$

where [Si], etc., is the weight percentage of the elements present. He has defined $M_{D\ 30}$ arbitrarily as the temperature at which 50% martensite is formed in tension after a true strain of 0.30. As a result austenite is most unstable for the lowest alloy content. The effect of carbon and molybdenum can be interpreted on this basis. As can be seen in Fig. 8, elongation first increases with carbon and then attains a maximum in the range of 0.2 to 0.3% carbon beyond which it drops.

At low carbon, austenite stability is very low and as a result martensite forms at a lower value of strain while at a higher carbon, austenite being more stable, martensite forms during the later stage and thereby favorably inhibits necking giving rise to a higher elongation. But when the carbon content exceeds the limit of solubility, the beneficial effect of increased carbon is lost since the undissolved carbides make the steel brittle. This is thought to be the reason for the low ductility in alloys with 0.45 or higher carbon alloys in the present investigation.

The effect of molybdenum on yield strength and elongation is shown

in Fig. 28. The higher yield strength of 4% Mo alloy compared to that of 1% Mo can be explained on the basis of solid solution strengthening effect of Mo in Fe. The decrease in elongation can be explained on the basis of a lower strain hardening associated with the higher Mo alloys due to higher austenite stability.

3.4.2 Effect of Composition on Strain Hardening Characteristics of the Steels

Figure 15 shows the effect of carbon on the strain hardening exponent at different temperatures for the fully annealed alloys. Figures 16-19 shows the same for the alloys after 80% deformation at the various temperatures as indicated. It is obvious that except for the 0.05 C alloy, the value of n does not change much with carbon in the range studied. The lower value of n for the 0.05 C alloy (alloy j) is much more prominent after processing. As discussed in the previous section, this alloy is martensitic initially and as the amount of martensite formed on subsequent testing is smaller in this alloy than in other alloys. Also this alloy has a higher molybdenum than the others. Molybdenum causes a decrease in strain hardening exponent as seen by Fig. 28 due to the increased austenite stability associated with molybdenum as discussed in the previous section. Therefore, the lower value of n face alloy j (0.05 C) can be attributed either to its higher molybdenum content or to its being martensitic prior to testing or both.

3.5 Effect of Process Variables on Properties

The main processing variables in any thermo-mechanical process are the temperature and amount of deformation. Due to the similarity of the present process to ausforming, the effect of processing variables is

expected to be similar in both cases. The effect on mechanical properties of increasing the amount of prior deformation at a constant temperature of deformation has been discussed by Zackay et al.[14] and Fahr.[19] Due to the fact that strain hardening is also expected to be affected by process variables, it was also studied in detail in the present investigation.

3.5.1 Effect of Processing Variables on the Strength and Ductility of Steels

Since it was reported by Zackay et al.[14] that the best properties of these steels are obtained after 80% deformation above M_D temperature, most of the investigation was on materials in this condition. Some alloys were deformed only 20% and the results are shown in Table XIV. As shown in Fig. 29, the yield strength goes up with increasing amount of prior deformation as expected. The increase is much more pronounced at low amounts of deformation. Additional increases in the amount of deformation do increase the yield strength but at a lower rate.

The effect of temperature of deformation can be only roughly established from the existing data. Figures 25 and 26 show that when the temperature of deformation is increased from 250°C to 350°C, the strength goes down. When the temperature is increased from 350°C to 450°C, the strength goes up and on further increasing the temperature of deformation to 550°C, the strength shows a drop. The results indicate that the best properties are obtained after 80% deformation at 450°C for 0.28 carbon content. A yield strength of 223,000 psi with an elongation of 31% was obtained.

At a temperature of deformation below M_D, the alloy transforms to martensite on processing. As a result ductility is completely lost as

shown in Tables III and IV for the alloys deformed at 25°C. At a temperature of deformation not much above M_D, the diffusivity is inadequate for precipitation to occur. Thus strengthening is limited only to the contribution due to the work hardening of material during rolling. This is thought to be the case for those deformed 80% at 250°C and 350°C. The higher yield strength for those deformed 80% at 250°C than those at 350°C can be associated with higher work hardening during rolling at 250°C than that at 350°C. As said earlier, 450°C is found to be the optimum temperature of deformation. Above this temperature, recovery, coarsening of the precipitates and eventually recrystallization, occur with the resultant loss of strength.[19] This effect is quite obvious from Figs. 25 and 26 and Table XV. On increasing the temperature of deformation from 450°C to 650°C, the yield strength drops from 222,000 psi to 173,000 psi.

In addition to the above treatments, a slightly more complex rolling schedule was carried out on a number of samples. Specimens which had been processed above their M_D temperatures and had yield strengths above 200,000 psi and elongation of 25-35 % were subjected to additional straining below their M_D temperature and tempered. The properties of these specimens are shown in Tables IX-XI. Table XI shows that excellent combinations of strength and ductility were obtained. The yield strength is in the range of 290-310,000 psi with elongations of 20-22% in most of the cases.

A good combination of strength and ductility was also obtained by deforming small amounts at a temperature somewhat above M_D temperature followed by tempering as shown in Tables XII and XIII.

3.5.2 Effect of Processing Variables on Strain Hardening Characteristics of the Steels

The effect of various processing conditions on the strain hardening exponent can be seen from Tables II-VIII. Figure 27 shows the variation of strain hardening exponent, n, with the temperature of deformation at two different test temperatures. Changing deformation temperatures above M_D does not seem to have a significant effect on the value of n. The amount of prior deformation has a considerable influence on the characteristics of the steels. This is obvious when changes in the nature of load-extension curves with the amount of prior deformation are followed. The shape of the load-extension curve for no prior deformation is characteristic of stable austenite which is shown as type I in Fig. 2. At a lower prior deformation, serrations appear as shown for type VIII A in Fig. 2. At 80% deformation, a well defined yield point is developed with a large amount of Lüders' strain. At strains in excess of the Lüders' strain, the slope of the load extension curve is very steep. The curves are shown schematically in Fig. 2 as types IV-VI.

As a result, after 80% deformation the value of n is much different than that after 20% deformation.

4. SUMMARY AND CONCLUSIONS

The effects of thermo-mechanical treatments on the strength, ductility and strain hardening characteristics of metastable austenitic steels have been investigated. The strength, ductility, and strain hardening exponent was determined as a function of testing temperature and carbon content. The results have been discussed on the basis of individual and combined effects of composition, test temperature and temperature of deformation on the martensitic reaction which the metastable austenitic steels undergo during straining. The tensile strength and strain hardening rate of metastable austenitic steels decrease as the amount of martensite formed during testing decreases. Increasing the testing temperature decreases the amount of martensite formed and hence decreases the tensile strength and strain hardening rate. Tensile elongation also depends on the amount of martensite formed during testing. The formation of martensite inhibits incipient necking. As a result only the martensite formed during the later stages of testing is beneficial. The idea that only the martensite formed during necking is beneficial is supported by the fact that alloys with 0.2-0.3 carbon or those tested at 100°C exhibit higher elongation since in other cases the austenite is either highly stable or highly unstable.

The results obtained may be summarized as follows:

(1) The strength and ductility were found to be strongly dependent on carbon content of the steels, because of the effect of carbon on austenite-martensite transformation. Carbon in the range of 0.2-0.3 was found to give best combinations of strength and ductility.

(2) In the case of higher carbon steels (0.4 or 0.5), a lower Mo gives higher ductility but lower yield strength.

(3) Test temperature directly affects the amount of martensite formed during testing and hence elongation. The highest elongations were found at 100°C in most cases.

(4) The strain hardening exponent was found to be strongly dependent on the test temperature. The effect was more pronounced for the case of processed alloys than in fully annealed alloys. Except for the lower range, carbon does not seem to have significant effects on the strain hardening exponent of these alloys.

(5) In many cases, serrated load-extension curves were obtained. The serrations were attributed to the martensite formation.

(6) In the case of the alloys deformed 80% at temperatures above M_D and tested at 22°C or below, the load extension curve showed a marked yield point, large Lüders' strain followed by a steep rise in the curve.

(7) Metastable austenitic steels having yield strengths in the range of 200,000 to 300,000 psi with 30 to 20% elongation have been obtained by certain thermo-mechanical processes.

(8) These steels retain their mechanical properties in the range of -196°C to 100°C. At a testing temperature of 200°C, they lose their ductility due to the absence of martensitic transformation.

(9) The best properties were obtained for steels with 0.2-0.3 carbon content after 80% deformation at 450°C.

ACKNOWLEDGMENTS

The author is deeply grateful to Professor E. R. Parker, Professor V. F. Zackay and Dr. Dan Merz for their guidance, encouragements and support throughout the course of this investigation.

This work was performed under the auspices of the United States Atomic Energy Commission.

REFERENCES

1. V. F. Zackay and E. R. Parker, High Strength Materials, V. F. Zackay, Ed., (John Wiley and Sons, Inc., New York, 1965), p. 130.
2. J. E. Bailey, Electron Microscopy and Strength of Crystals, G. Thomas and J. Washburn, Eds., (Interscience Publications, New York, 1963), p. 535.
3. R. H. Busch, ASM, 56, 885 (1963).
4. G. Thomas, D. Schmatz and W. W. Gerberich, High Strength Materials, V. F. Zackay, Ed., (John Wiley and Sons, Inc., New York, 1965), p. 251.
5. V. F. Zackay, W. W. Gerberich, R. Busch and E. R. Parker, Int. J. Fracture Mechanics, 2, 638 (1966).
6. B. Cina, JISI, 177, No. 4, 406 (1954).
7. R. A. Lincoln and W. H. Mather, Regional Technical Meeting, Iron and Steel Inst., (1948) 57.
8. W. D. Binder, Metal Prog. 201 (1950).
9. W. M. Justusson and D. J. Schmatz, Trans. ASM, 55, 640 (1962).
10. H. C. Doepken, Trans. AIME, 194, 166 (1952).
11. C. D. Starr, Trans. AIME, 197, 654 (1952).
12. N. A. Ziegler and P. H. Brace, Proc. ASM, 50, 861 (1950).
13. A. W. McReynolds, J. Appl. Phys. 20, 896 (1949).
14. V. F. Zackay, E. R. Parker, D. Fahr and R. Busch, Trans. ASM, 60, 262 (1967).
15. J. Bressanelli and A. Moskowitz, Trans. ASM, 59, 223 (1966).
16. G. E. Dieter, Jr., Mechanical Metallurgy, (McGraw-Hill Book Company, New York, 1961).

17. T. Angel, JISI, 177, 165 (1954).

18. J. S. Dunning, M.S. Thesis, University of California, Berkeley, (December 1966).

19. D. Fahr, M.S. Thesis, University of California, Berkeley, (June 1966).

20. B. R. Banerjee, J. M. Capenos, J. J. Hauser, Application of Fracture Toughness Parameters to Structural Metals, (Gordon and Breach, 1966).

21. W. W. Gerberich, C. F. Martin and V. F. Zackay, Trans. ASM, 58, 85 (1965).

22. F. R. Larson and J. Nunes, Trans. ASM, 53, 663 (1966).

23. G. W. Powell, E. R. Marshall and W. A. Backofen, Trans. ASM, 50, 478 (1958).

FIGURE CAPTIONS

Fig. 1 Tensile specimens used in the determination of mechanical properties.

(a) Long gauge tensile specimen with gauge length 1" and thickness 0.05".

(b) Short gauge tensile specimen with gauge length 0.5" and thickness 0.05".

Fig. 2 Schematic diagram of the types of load-extension curves obtained.

Fig. 3 Yield strength and elongation is testing temperature in °C for different alloys as indicated in annealed condition.

Fig. 4 Yield strength and elongation vs testing temperature in °C for different alloys as indicated after 80% deformation at 250°C.

Fig. 5 Yield strength and elongation vs testing temperature in °C for different alloys as indicated after 80% deformation at 350°C.

Fig. 6 Yield strength and elongation vs testing temperature in °C for different alloys as indicated after 80% deformation at 450°C.

Fig. 7 Yield strength and elongation vs testing temperature in °C for different alloys as indicated after 80% deformation at 550°C.

Fig. 8 Yield strength and elongation at room temperature vs % carbon in the alloys after 80% deformation at various temperatures as indicated.

Fig. 9 Yield strength and elongation at liquid nitrogen vs % carbon in the alloys after 80% deformation at various temperatures as indicated.

Fig. 10 Strain hardening exponent, n, vs testing temperature in °C for different alloys as indicated in annealed condition.

Fig. 11 Strain hardening exponent, n, vs testing temperature in °C for different alloys as indicated after 80% deformation at 250°C.

Fig. 12 Strain hardening exponent, n, vs testing temperature in °C for different alloys as indicated after 80% deformation at 350°C.

Fig. 13 Strain hardening exponent, n, vs testing temperature in °C for different alloys as indicated after 80% deformation at 450°C.

Fig. 14 Strain hardening exponent, n, vs testing temperature in °C for different alloys as indicated after 80% deformation at 550°C.

Fig. 15 Strain hardening exponent, n, at various test temperatures as indicated vs % carbon in the annealed alloys.

Fig. 16 Strain hardening exponent, n, at various test temperatures as indicated vs % carbon in the alloys after 80% deformation at 250°C.

Fig. 17 Strain hardening exponent, n, at various test temperatures as indicated vs % carbon in the alloys after 80% deformation at 350°C. The testing temperatures are indicated.

Fig. 18 Strain hardening exponent, n, at various test temperatures as indicated vs % carbon in the alloys after 80% deformation at 450°C. The testing temperatures are indicated.

Fig. 19 Strain hardening exponent, n, at various test temperatures as indicated vs % carbon in the alloys after 80% deformation at 550°C. The testing temperatures are indicated.

Fig. 20 (a),(b) Computer plots of true stress vs true strain and log time stress vs log time strain for

(a) the alloy k in annealed condition at -196°C.

(b) the alloy l in annealed condition at -196°C.

Fig. 21 (a),(b) Computer plots of true-stress vs true strain and log true stress vs log true strain for

(a) alloy k in annealed condition tested at 22°C

(b) alloy k in annealed condition tested at 100°C

Fig. 22 (a),(b) Computer plots of true-stress vs true strain and log true stress vs log true strain for

(a) alloy k after 80% deformation at 350°C and tested at -196°C

(b) alloy k after 80% deformation at 350°C and tested at -78°C.

Fig. 23 (a),(b) Computer plots of true-stress vs true strain and log true stress vs log true strain for

(a) alloy k after 80% deformation at 350°C and tested at 22°C

(b) alloy k after 80% deformation at 350°C and tested at 100°C

Fig. 24 Yield strength and elongation at various test temperatures vs strain hardening exponent, n, for different alloys as indicated after 80% deformation at 450°C.

Fig. 25 Yield strength and elongation at 22°C vs deformation temperature for different alloys as indicated after 80% deformation.

Fig. 26 Yield strength and elongation at -196°C vs deformation temperature for different alloys as indicated after 80% deformation.

Fig. 27 Strain hardening exponent, n, at 22°C and -196°C vs deformation temperature for different alloys as indicated after 80% deformation.

Fig. 28 Elongation, strain hardening exponent, n, yield and tensile strength at 22°C vs molybdenum content of the alloys after 20% deformation at 450°C.

Fig. 29 Yield and tensile strength at 22°C vs amount of deformation at various temperatures and alloys as indicated.

Table I Chemical composition of the alloys

Alloy Identification No.	Ingot No.	Cr	Ni	Mn	Si	Mo	C	Fe
a	673-10	9.54	7.20	3.18	1.75	1.10	0.51	Balance
b	673-11	8.54	7.23	2.44	1.83	4.03	0.52	Balance
c	674-9	8.81	7.48	1.47	1.87	3.92	0.35	Balance
d	674-10	8.81	7.48	1.41	1.81	3.93	0.45	Balance
e	674-11	8.79	7.51	1.40	1.91	3.99	0.51	Balance
f	674-13	9.46	7.47	2.42	1.87	1.10	0.43	Balance
g	674-14	8.86	7.53	2.32	1.90	4.07	0.43	Balance
h	676-1	8.90	7.50	2.90	2.80	4.00	0.28	Balance
i	6691	8.88	7.60	2.08	1.96	4.04	0.25	Balance
j	6698-1	12.23	7.69	0.68	1.6	4.10	0.05	Balance
k	6698-2	11.64	7.69	0.60	1.3	2.5	0.07	Balance
l	6698-3	11.84	7.71	0.61	1.5	3.0	0.16	Balance
m	6698-4	11.99	7.71	0.52	0.7	3.2	0.20	Balance

Table II. Properties of annealed alloys after reducing 80% at 450°C.*

Property / Test Temp.	% of Carbon	Alloy Identification No.	Y.S. $\times 10^3$ psi	T.S. $\times 10^3$ psi	T.S / Y.S.	% elongation	Strength coefficient, A	Strain Hardening exponent, n	Magnetic** characteristic		Type of Load/Extension curve
									Before test	After test	
-196°C	0.05	j	64	289	4.5	23	4.56	0.75	M	M	I
	0.07	k	48	309	6.4	20	4.73	0.77	M'	M	I
	0.16	l	78	248	3.2	24	4.35	0.84	A	M	IA
	0.20	m	87	257	3.0	24	4.23	0.95	A	M	IA
-78°C	0.05	j	52	195	3.8	30	4.37	0.75	M'	M	IA
	0.07	k	39	213	5.5	26	4.35	0.86	A	M	IA
	0.16	l	61	213	3.5	44	4.29	0.78	A	M	IA
	0.20	m	68	222	3.2	48	4.18	0.87	A	M	IA
22°C	0.05	j	42	140	3.4	38	4.29	0.67	A	M	VIIA
	0.07	k	37	158	4.3	30	4.30	0.74	A	M	VIIA
	0.16	l	50	141	2.8	64	4.61	0.40	A	M	VII
	0.20	m	48	133	2.8	59	4.49	0.48	A	M	VII
100°C	0.05	j	32	83	2.6	49	4.46	0.38	A	M	VII
	0.07	k	28	79	2.8	40	4.46	0.36	A	M'	VII
	0.16	l	35	90	2.5	66	4.44	0.41	A	M'	VII
	0.20	m	37	94	2.6	62	4.57	0.34	A	M''	VII
200°C	0.05	j	25	74	3.0	40	4.33	0.44	A	M''	VII
	0.07	k	22	70	3.2	44	4.31	0.44	A	M''	VII
	0.16	l	28	78	2.8	46	4.33	0.46	A	A	VII
	0.20	m	28	80	2.9	43	4.40	0.42	A	A	VII

* Specimen (a), 1" Gauge Length.

** M = Magnetic, M' = Slightly magnetic, M'' = very slightly magnetic, A = Non-magnetic

Table III. Properties of Alloys after 80% deformation at 25°C*.

Property / Test Temp.	% of Carbon	Alloy Identification No.	Y.S. $\times 10^3$ psi	T.S. $\times 10^3$ psi	T.S / Y.S.	% elongation	Strength coefficient, A	Strain Hardening exponent, n	Magnetic characteristic** Before test	Magnetic characteristic** After test	Type of Load/Extension curve
-196°C	0.05	j	320	320	1.0	3	——	——	M	M	IIA
	0.07	k	362	362	1.0	2	——	——	M	M	IIA
	0.16	l	386	386	1.0	1	——	——	M	M	IIA
	0.35	c***	465	465	1.0	0	——	——	M	M	III
-78°C	0.05	j	258	258	1.0	3	——	——	M	M	IIA
	0.07	k	312	312	1.0	2	——	——	M	M	IIA
	0.16	l	318	318	1.0	2	——	——	M	M	IIA
22°C	0.05	j	225	225	1.0	2	——	——	M	M	IIA
	0.07	k	266	266	1.0	1	——	——	M	M	IIA
	0.16	l	290	290	1.0	2	——	——	M	M	IIA
	0.35	c***	359	359	1.0	0	——	——	M	M	III
100°C	0.05	j	231	231	1.0	2	——	——	M	M	IIA
	0.07	k	269	269	1.0	1	——	——	M	M	IIA
	0.16	l	294	294	1.0	2	——	——	M	M	IIA
200°C	0.05	j	223	223	1.0	1	——	——	M	M	IIB
	0.07	k	260	260	1.0	1	——	——	M	M	IIB
	0.16	l	282	282	1.0	2	——	——	M	M	IIB

* Specimen (a), 1" Gauge Length.

** M = Magentic, M' = Slight magnetic, M" = very slightly magnetic, A = Non-magnetic.

*** Deformed 75% instead of 80%.

Table IV. Properties of alloys after 80% deformation at 25°C, by tempering one hour at 450°C*.

Property / Test Temp.	% of Carbon	Alloy Identification No.	Y.S. $\times 10^3$ psi	T.S. $\times 10^3$ psi	T.S / Y.S.	% elongation	Strength coefficient, A	Strain Hardening exponent, n	Magnetic** characteristic Before test	Magnetic** characteristic After test	Type of Load/Extension curve
-196°C	0.05	j	386	386	1.0	2	—	—	M	M	IIA
	0.07	k	407	407	1.0	0	—	—	M	M	III
	0.16	l	425	425	1.0	1	—	—	M	M	IIA
-78°C	0.05	j	322	322	1.0	2	—	—	M	M	IIA
	0.07	k	355	355	1.0	1	—	—	M	M	IIA
	0.16	l	367	367	1.0	2	—	—	M	M	IIA
22°C	0.05	j	298	298	1.0	2	—	—	M	M	IIA
	0.07	k	331	331	1.0	0	—	—	M	M	III
	0.16	l	337	337	1.0	1	—	—	M	M	IIA
100°C	0.05	j	274	274	1.0	2	—	—	M	M	IIA
	0.07	k	309	309	1.0	1.	—	—	M	M	IIA
	0.16	l	321	321	1.0	2	—	—	M	M	IIA
200°C	0.05	j	260	260	1.0	2	—	—	M	M	IIA
	0.07	k	283	283	1.0	2	—	—	M	M	IIB
	0.16	l	297	297	1.0	1	—	—	M	M	IIB

* Specimen (a), 1" Gauge Length.

** M = Magnetic, M' = Slightly magnetic, M" = Very slight magnetic, A = Non-magnetic.

Table V. Properties of alloys after 80% deformation at 250°C*.

Property / Test Temp.	% of Carbon	Alloy Identification No.	Y.S. $\times 10^3$ psi	T.S. $\times 10^3$ psi	T.S / Y.S.	% elongation	Strength coefficient, A	Strain Hardening exponent, n	Magnetic characteristic** Before test	Magnetic characteristic** After test	Type of Load/Extension curve
-196°C	0.05	j	194	315	1.6	22	4.67	0.74	M'	M	IV
	0.07	k	186	322	1.7	18	4.39	0.99	M'	M	IV
	0.16	l	191	330	1.7	18	4.35	0.95	A	M	IV
	0.20	m	209	346	1.7	19	4.52	0.91	A	M	IV
-78°C	0.05	j	136	235	1.7	16	4.88	0.52	M'	M	VI
	0.07	k	142	251	1.8	19	4.81	0.57	M'	M	VI
	0.16	l	163	261	1.6	20	4.85	0.56	A	M	VI
	0.20	m	170	267	1.6	21	4.83	0.57	A	M	VI
22°C	0.05	j	131	192	1.5	17	4.95	0.37	M'	M	VI
	0.07	k	148	206	1.4	19	4.96	0.36	M''	M	VI
	0.16	l	161	214	1.3	22	4.97	0.35	A	M	VI
	0.20	m	191	227	1.2	26	4.97	0.37	A	M	VIII
100°C	0.05	j	168	170	1.01	23	5.13	0.13	M'	M	X
	0.07	k	193	193	1.0	23	5.14	0.18	M''	M	X
	0.16	l	190	190	1.0	23	5.25	0.10	A	M	X
	0.20	m	209	209	1.0	17	5.24	0.11	A	M	X
200°C	0.05	j	174	174	1.0	4	——	——	M'	M	II
	0.07	k	175	175	1.0	5	——	——	M''	M	II
	0.16	l	179	179	1.0	5	——	——	A	M'	II
	0.20	m	186	186	1.0	4	——	——	A	M'	II

* Specimen (a), 1" Gauge Length

** M = Magnetic, M' = Slightly magnetic, M'' = Very slightly magnetic, A = Non-magnetic.

Table VI. Properties of alloys after 80% deformation at 350°C*.

Property / Test Temp.	% of Carbon	Alloy Identification No.	Y.S. $\times 10^3$ psi	T.S. $\times 10^3$ psi	T.S / Y.S.	% elongation	Strength coefficient, A	Strain Hardening exponent, n	Magnetic characteristic** Before test	Magnetic characteristic** After test	Type of Load/Extension curve
-196°C	0.05	j	177	327	1.9	20	4.47	0;93	M	M	IV
	0.07	k	174	344	2.0	22	4.43	0.97	M'	M	IV
	0.16	l	179	348	1.9	19	4.48	0.94	A	M	IV
	0.20	m	189	328	1.7	14	4.21	1.21	A	M	IV
	0.35	c***	205	237	1.2	9	4.71	0.74	A	M	IV
-78°C	0.05	j	125	219	1.7	17	4.84	0.53	M	M	VI
	0.07	k	139	241	1.7	18	4.84	0.54	M'	M	VI
	0.16	l	147	250	1.7	20	4.77	0.60	A	M	VI
	0.20	m	145	259	1.8	15	4.74	0.69	A	M	VI
22°C	0.05	j	128	177	1.4	18	4.91	0.36	M	M	VI
	0.07	k	144	205	1.4	20	4.91	0.40	A	M	VI
	0.16	l	149	213	1.4	19	4.51	0.41	A	M	VIA
	0.20	m	156	215	1.4	20	4.87	0.44	A	M	VIA
	0.35	c***	212	248	1.2	16	5.01	0.38	A	M	V
100°C	0.05	j	150	152	1.02	23	5.08	0.13	M	M	X
	0.07	k	167	175	1.1	35	5.07	0.19	A	M	X
	0.16	l	174	179	1.03	34	5.13	0.15	A	M	X
	0.20	m	182	190	1.04	29	5.17	0.14	A	M	X
200°C	0.05	j	158	158	1.0	4	—	—	M	M	II
	0.07	k	166	166	1.0	5	—	—	A	M"	II
	0.16	l	175	175	1.0	5	—	—	A	M"	II
	0.20	m	183	183	1.0	5	—	—	A	M"	II

* Specimen (a), 1" Gauge Length.

** M = Magnetic, M' = Slight magnetic, M" = Very slightly magnetic, A = Non-magnetic.

*** Deformed 75% instead of 80%

Table VII. Properties of alloys after 80% deformation at 450°C.*

Property / Test Temp.	% of Carbon	Alloy Identification No.	Y.S. $\times 10^3$ psi	T.S. $\times 10^3$ psi	T.S / Y.S.	% elongation	Strength coefficient, A	Strain Hardening exponent, n	Magnetic** characteristic		Type of Load/Extension curve
									Before test	After test	
-196°C	0.05	j	187	235	1.3	12	4.71	0.69	M	M	V
	0.07	k	169	322	1.9	23	4.27	1.09	M'	M	IV
	0.16	l	174	348	2.0	24	4.59	0.81	A	M	IV
	0.2	m	188	361	1.9	25	4.58	0.85	A	M	IV
	0.28	i	221	286	1.3	13	4.50	0.93	A	M	V
	0.35	c***	194	231	1.2	9	4.44	1.07	A	M	V
	0.45	d***	209	253	1.2	9	4.78	0.71	A	M	V
-78°C	0.05	j	155	215	1.4	17	4.83	0.54	M	M	VI
0	0.07	k	142	236	1.7	20	4.65	0.71	A	M	VI
	0.16	l	142	248	1.8	21	4.69	0.69	A	M	VI
	0.20	m	146	254	1.7	19	4.71	0.68	A	M	VI
22°C	0.05	j	153	185	1.2	23	4.99	0.31	M	M	VIA
	0.07	k	150	199	1.3	22	4.81	0.47	M"	M	VIA
	0.16	l	153	210	1.4	24	4.89	0.41	A	M	VIA
	0.2	m	161	218	1.4	23	4.92	0.40	A	M	VIA
	0.28	h	223	241	1.1	31	4.89	0.42	A	M	VIII
	0.35	c***	196	271	1.4	17	4.88	0.52	A	M	V
	0.43	f	215	215	1.0	0.0	-	-	M	M	III
	0.45	d***	222	264	1.2	14	4.97	0.45	A	M	V
100°C	0.05	j	168	168	1.0	5	5.19	0.04	M	M	IX
	0.07	k	160	163	1.02	28	5.10	0.14	A	M	X
	0.16	l	181	183	1.01	28	5.18	0.12	A	M	X
	0.2	m	177	182	1.03	36	5.06	0.22	A	M	X
200°C	0.05	j	171	171	1.0	3	-	-	M	M	II
	0.07	k	162	162	1.0	4	-	-	A	M	II
	0.16	l	169	169	1.0	3	-	-	A	M"	II
	0.20	m	171	171	1.0	5	-	-	A	A	II

* Specimen (a), 1" gauge length

** M = Magnetic, M' = Slightly magnetic, M" = Very slightly magnetic, A = Non-magnetic

*** Deformed 75% instead of 80%

Table VIII. Properties of alloys after 80% deformation at 550°C*.

Property / Test Temp.	% of Carbon	Alloy Identification No.	Y.S. $\times 10^3$ psi	T.S. $\times 10^3$ psi	T.S / Y.S.	% elongation	Strength coefficient, A	Strain Hardening exponent, n	Magnetic characteristic** Before test	Magnetic characteristic** After test	Type of Load/Extension curve
-196°C	0.05	j	170	266	1.6	15	4.43	0.94	M	M	V
	0.07	k	176	279	1.6	15	4.34	1.06	A	M	V
	0.16	l	175	337	1.9	22	4.40	0.98	A	M	IV
	0.20	m	182	259	1.4	13	4.33	1.08	A	M	V
	0.35	c***	171	298	1.8	12	4.40	1.08	A	M	V
	0.45	d***	188	297	1.6	11	4.53	0.97	A	M	V
	0.51	e	239	240	1.0	0	—	—	A	M	III
-78°C	0.05	j	149	225	1.5	16	4.88	0.49	M	M	VI
	0.07	k	131	238	1.8	18	4.65	0.72	A	M	VI
	0.16	l	140	253	1.8	20	4.71	0.66	A	M	VI
	0.20	m	144	251	1.8	20	4.76	0.63	A	M	VI
22°C	0.05	j	161	191	1.2	19	4.98	0.32	M	M	VIA
	0.07	k	136	207	1.5	20	4.90	0.41	A	M	VI
	0.16	l	142	216	1.5	19	4.99	0.35	A	M	VIA
	0.20	m	157	225	1.8	23	4.90	0.42	A	M	VI
	0.35	c***	181	285	1.6	19	4.81	0.58	A	M	IV
	0.45	d***	202	292	1.4	18	4.80	0.61	A	M	IV
	0.51	f	216	248	1.2	15	4.90	0.48	A	M	VIIIA
	0.51	e	245	245	1.0	0	—	—	M	M	III
100°C	0.05	j	157	157	1.0	11	5.15	0.07	M	M	IX
	0.07	k	157	174	1.1	27	5.05	0.21	A	M	X
	0.16	l	151	176	1.2	35	5.05	0.21	A	M	X
	0.20	m	178	189	1.1	30	5.07	0.22	A	M	X
200°C	0.05	j	141	141	1.0	3	—	—	M	M	II
	0.07	k	148	148	1.0	6	—	—	A	M	II
	0.16	l	157	157	1.0	4	—	—	A	M'	II
	0.20	m	163	163	1.0	4	—	—	A	M''	II

* Specimen (a), 1" Gauge Length.

** M = Magnetic, M' = Slightly magnetic, M'' = Very slightly magnetic, A = Non-magnetic.

*** Deformed 75% instead of 80%

Table IX. Room temperature properties of alloy i after 50% deformation at 450°C plus 20% deformation at -196°C, plus tempering*.

Tempering Temp. °C	Tempering Time Minutes	Yield Strength $\times 10^3$ psi	Tensile Strength $\times 10^3$ psi	Hardness Rockwell, C (before test)	% Elongation
No Tempering		259	307	58	19
250	30	310	310	58	7
250	60	313	313	58	7
250	120	305	305	59	7
300	30	318	318	58	2
350	30	319	319	59	2
400	30	315	315	58	2
450	30	321	321	58	9
450	60	321	321	58	9

* Specimen (b), 0.5" Gauge Length, Magnetic before and after testing.

Table X. Room temperature properties of alloy i after 50% deformation at 450°C plus 20% deformation at 25°C, plus tempering*.

Tempering Temp. °C	Tempering time minutes	Yield Strength $\times 10^3$ psi	Tensile Strength $\times 10^3$ psi	Hardness Rockwell, C (before test)	% Elongation
No tempering		197	233	47	12
250	30	211	238	48	11
250	60	204	235	48	11
300	30	210	239	50	11
350	30	214	240	50	11
400	30	212	236	50	11
450	30	209	236	50	10
450	60	210	242	49	10

*Specimen (b), 0.5" Gauge length, slightly magnetic before and magnetic after testing.

Table XI Room temperature properties of alloy i after 75% deformation at 450°C plus 15% deformation at -196°C, plus tempering*

Tempering Temp. °C	Tempering Time Minutes	Yield Strength $\times 10^3$ psi	Tensile Strength $\times 10^3$ psi	Hardness Rockwell,C (before test)	% Elongation
No tempering		260	300	57	16
250	30	291	300	58	21
250	60	287	298	58	22
300	30	297	303	58	20
350	30	300	305	58	18
350	60	308	309	59	21
350	120	304	308	59	22
400	30	307	311	59	20
450	30	295	309	59	22
450	60	303	312	59	22
450	120	303	312	60	22

* Specimen (b), 0.5" gauge length, magnetic before and magnetic after testing.

Table XII Room temperature properties of alloy i after 27% deformation at 250°C followed by quenching to -196 C.*

Tempering Temp °C	Tempering Time Minutes	Yield Strength $\times 10^3$ psi	Tensile Strength $\times 10^3$ psi	Hardness Rockwell,C (before test)	% Elongation
Untempered		121	154	32	38
250	30	117	163	29	45
450	30	121	187	31	75

* Specimen (b), 0.5" gauge length, magnetic before and magnetic after testing

Table XIII Room temperature properties of alloy i after 15% deformation at 250°C followed by quenching to -196°C.*

Tempering Temp °C	Tempering Time Minutes	Yield Strength $\times 10^3$ psi	Tensile Strength $\times 10^3$ psi	Hardness Rockewell, C (before test)	% Elongation
Untempered		103	141	30	36
450	30	111	183	33	73

* Specimen (b), 0.5" gauge length, non-magnetic before and magnetic after testing.

Table XIV. Room temperature properties of alloys after 20% deformation at 450°C*.

% of Carbon	Alloy Identification No.	Y.S. $\times 10^3$ psi	T.S. $\times 10^3$ psi	$\frac{T.S}{Y.S.}$	% elongation	Strength coefficient, A	Strain Hardening exponent, n	Magnetic** characteristic		Type of Load/Extension curve
								Before test	After test	
0.43	f	141	182	1.2	25	5.08	0.18	A	M	VIIIA
0.43	g	162	178	1.1	17	5.18	0.10	A	M	VIIIA
0.51	a	132	174	1.3	20	5.07	0.19	A	M	VIIIA
0.52	b	155	182	1.1	12	5.17	0.12	A	M	VIIIA

* Specimen (a), 1" Gauge length.

** M = Magnetic, A = Non-magnetic.

Table XV Room temperature properties of alloy d after 75% deformation*

% of Carbon	Temperature of Deformation	Yield Strength $\times 10^3$ psi	Tensile Strength $\times 10^3$ psi	$\frac{T.S.}{Y.S.}$	% of Elongation
0.45	450	222	264	1.2	14
0.45	550	202	292	1.4	18
0.45	650	173	220	1.3	3

* Specimen (a), 1" gauge length

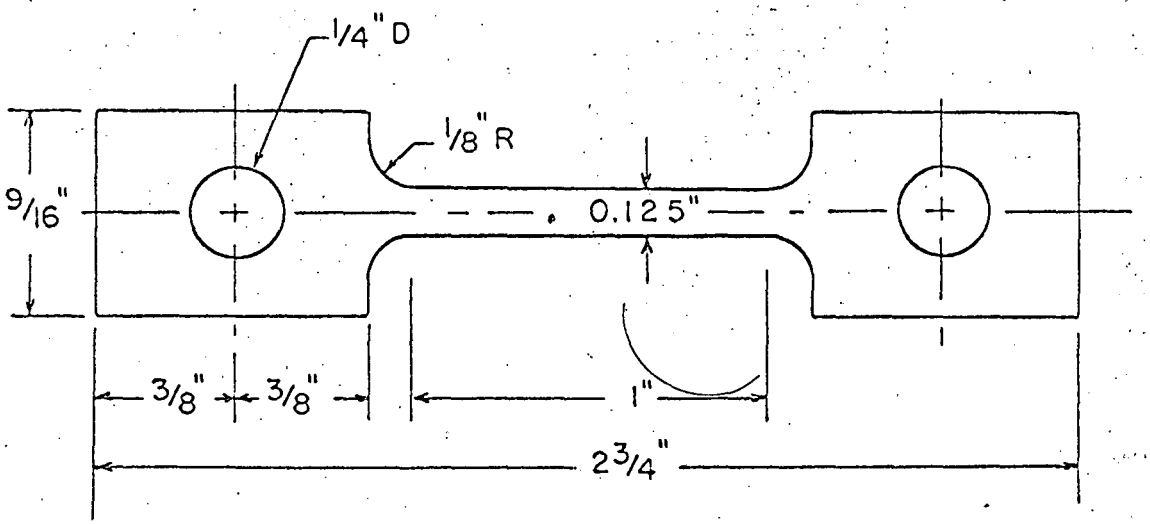

TENSILE SPECIMEN, a.
GAUGE LENGTH 1"; THICKNESS 0.05".
SCALE: 2" = 1"

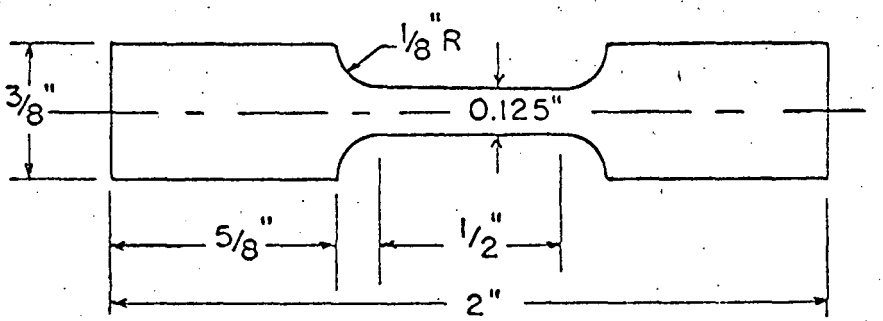

TENSILE SPECIMEN, b.
GAUGE LENGTH 1/2"; THICKNESS 0.05".
SCALE: 2" = 1"

XBL 678-4837

Fig. 1

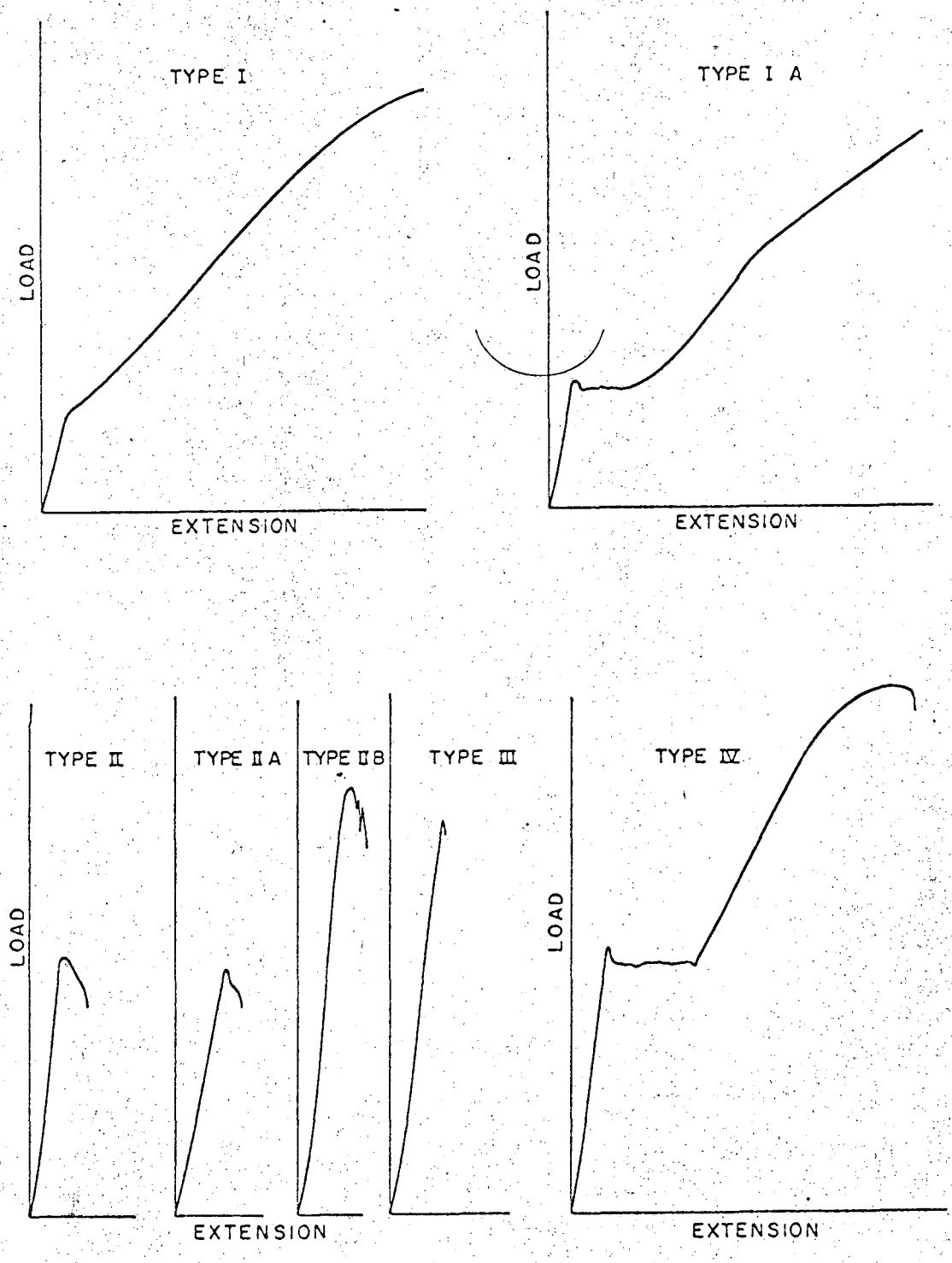
TYPE I
LOAD
EXTENSION
TYPE I A
LOAD
EXTENSION
TYPE II
TYPE II A
TYPE II B
TYPE III
LOAD
EXTENSION
TYPE IV
LOAD
EXTENSION
XBL 678-4333

Fig. 2

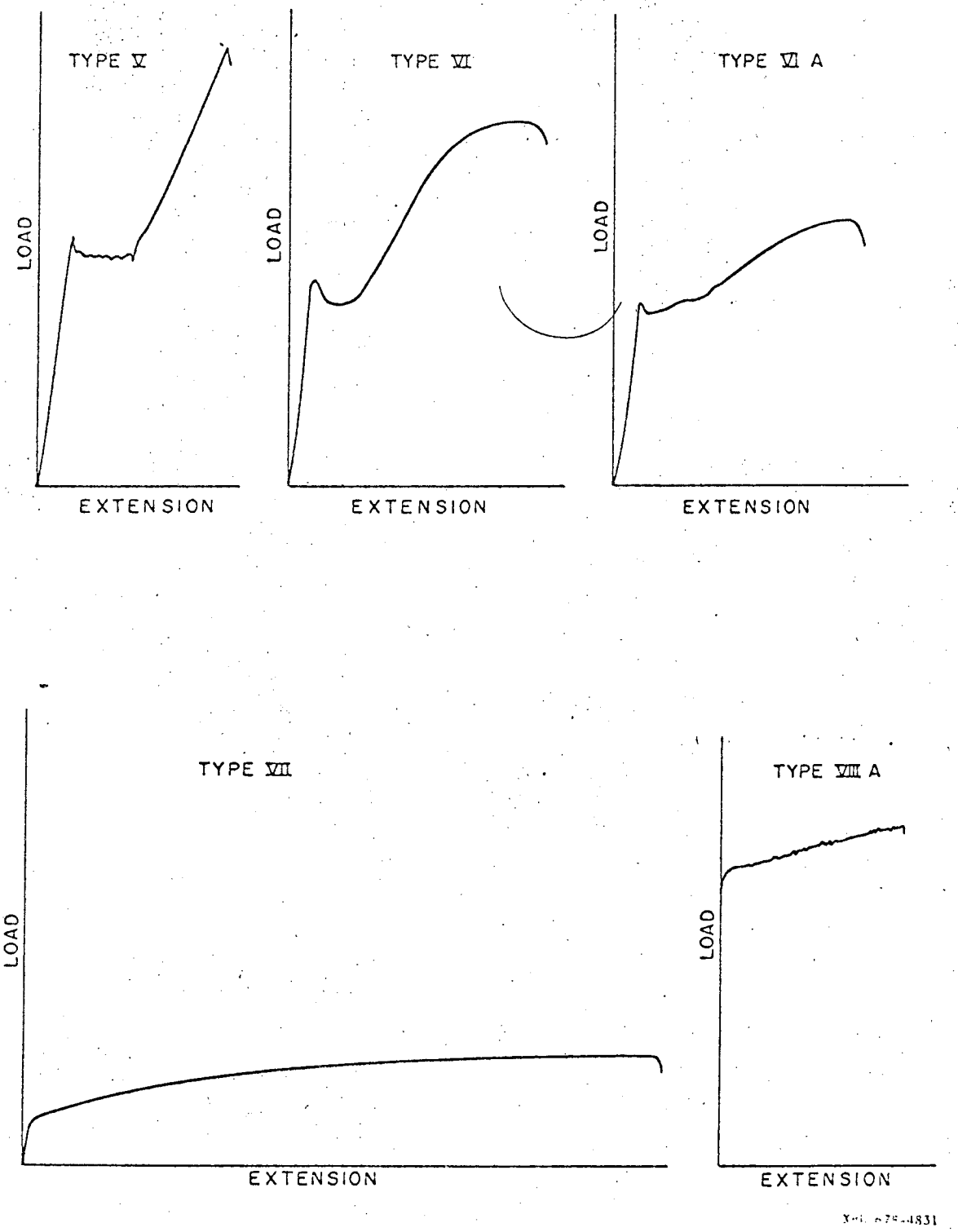

Fig. 2 (continued)

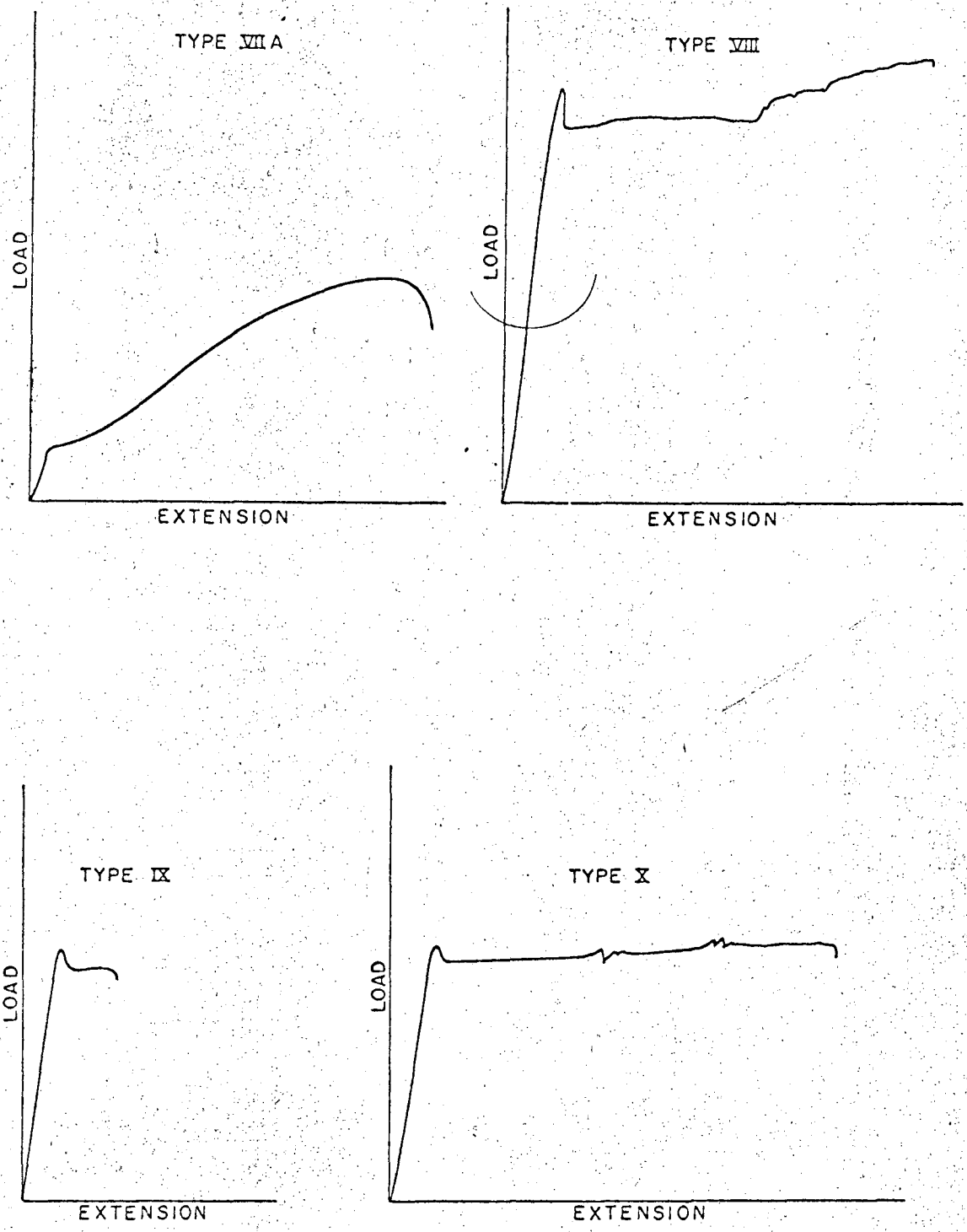

Fig. 2 (continued)

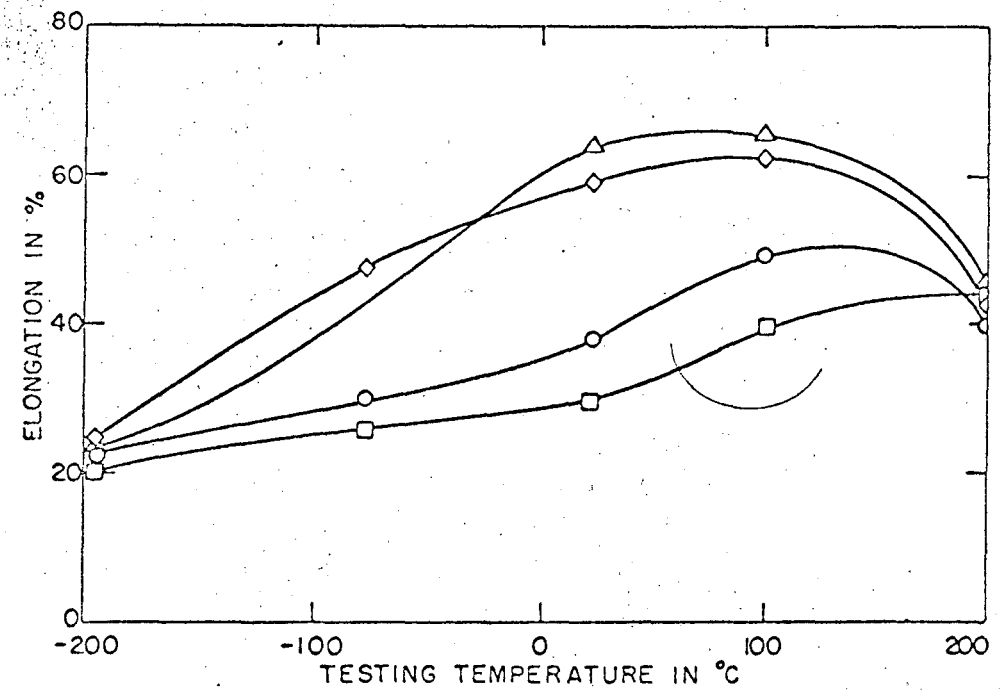

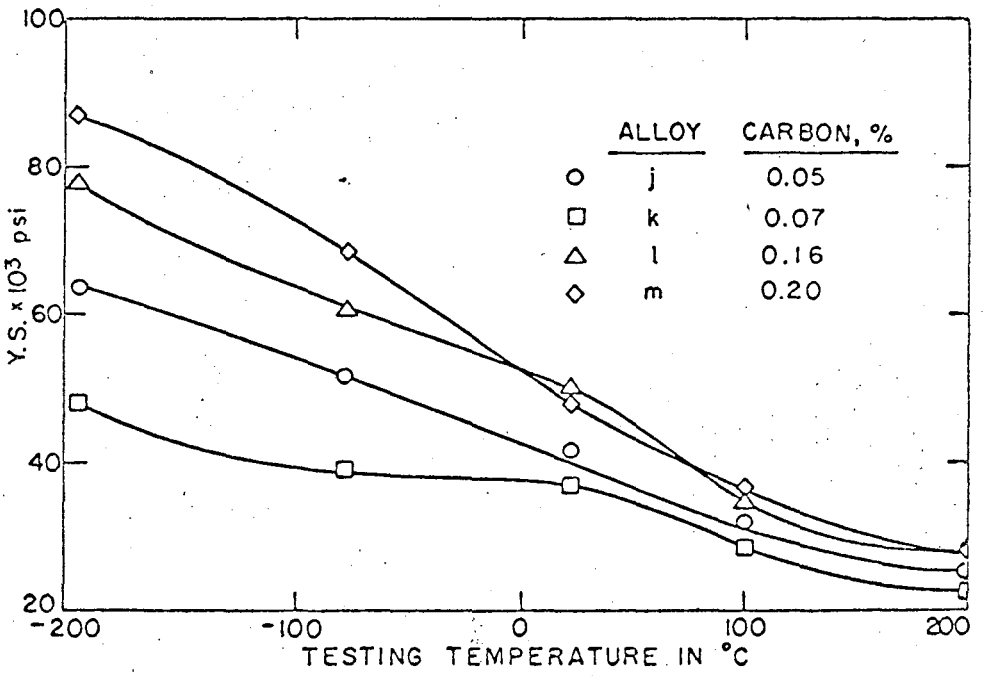

XBL 678-4828

Fig. 3

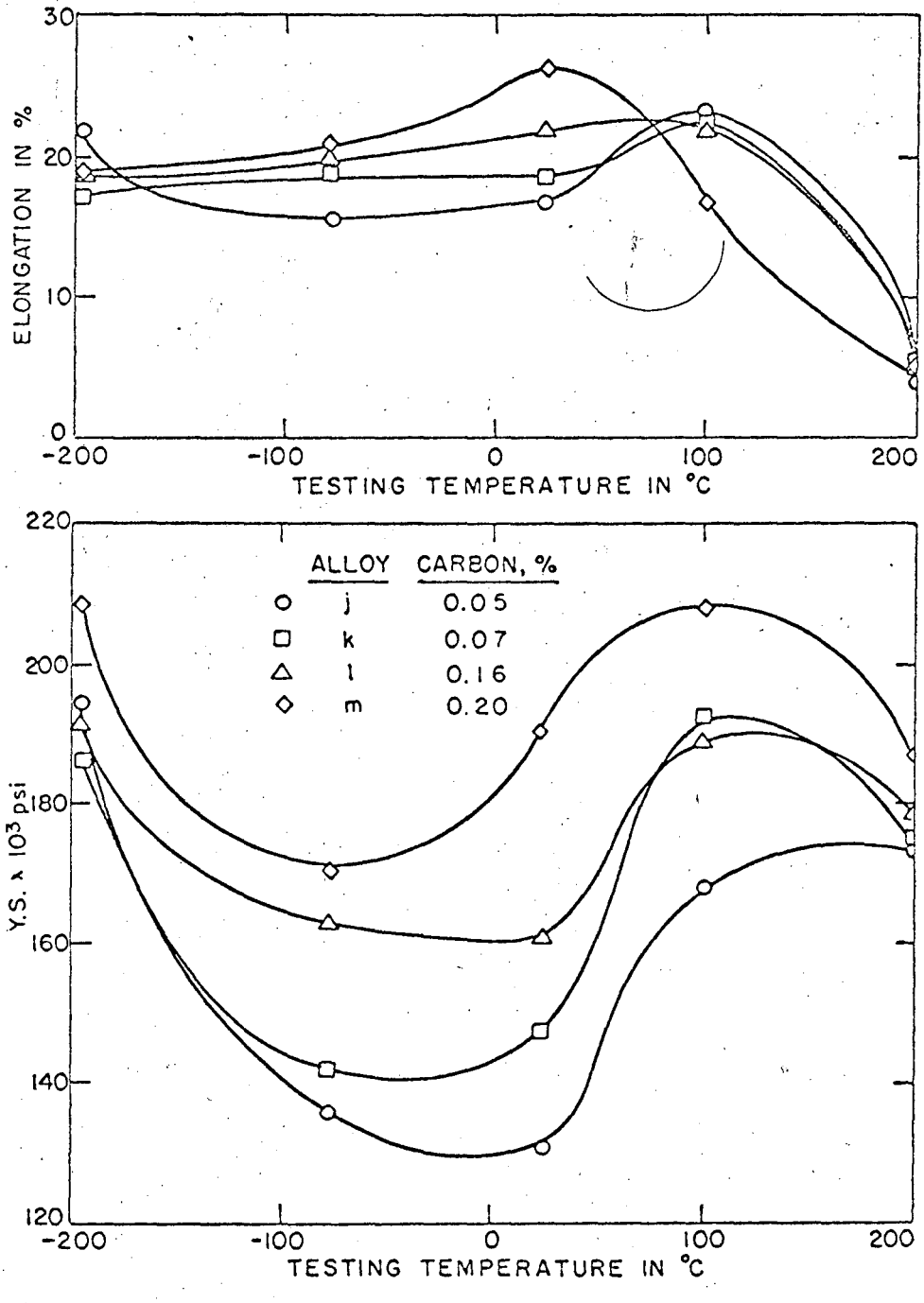

XBL 678-4826

Fig. 4

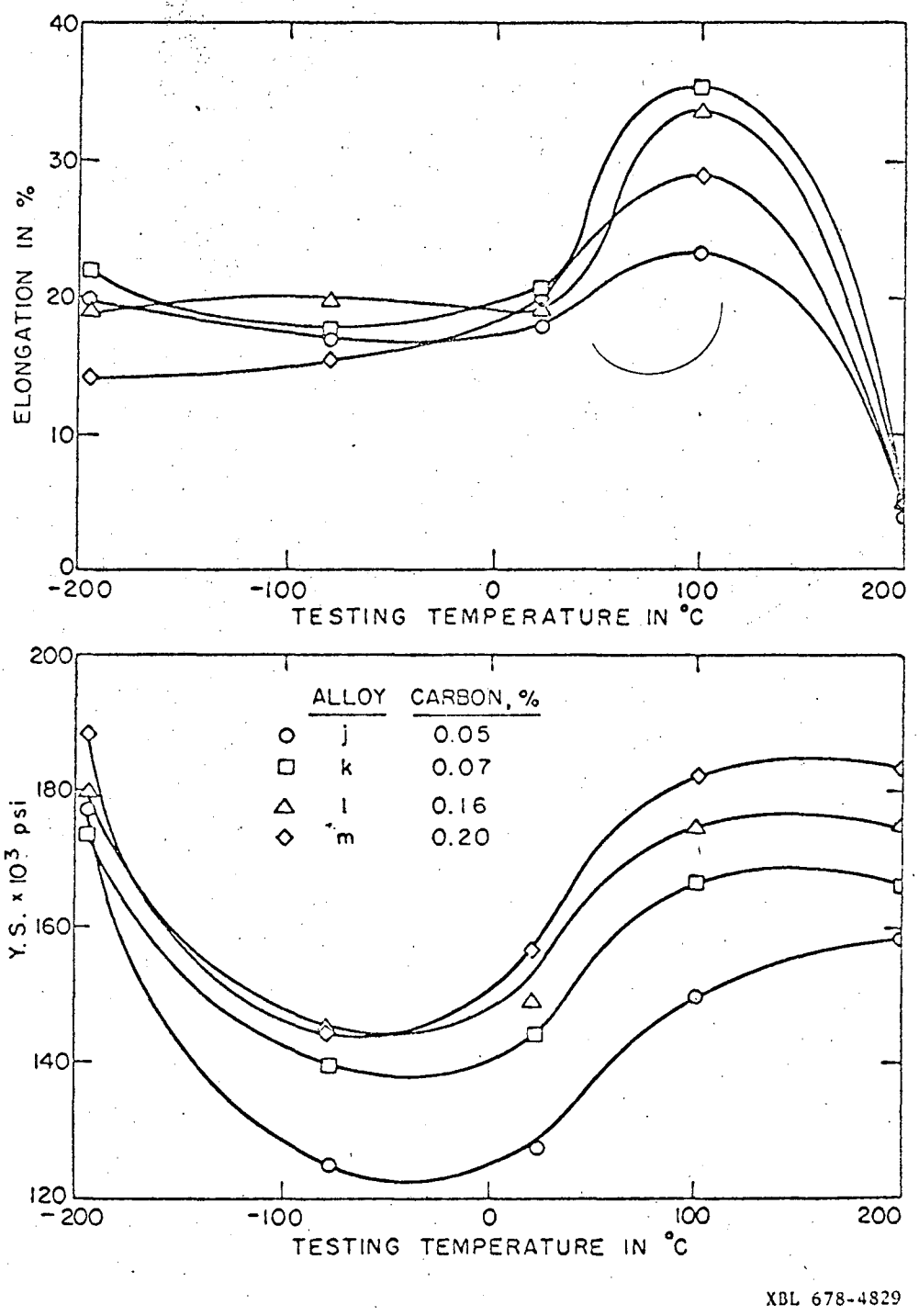
ELONGATION IN %
TESTING TEMPERATURE IN °C
Y.S. x 10³ psi
ALLOY CARBON, %
j 0.05
k 0.07
l 0.16
m 0.20
TESTING TEMPERATURE IN °C
XBL 678-4829

Fig. 5

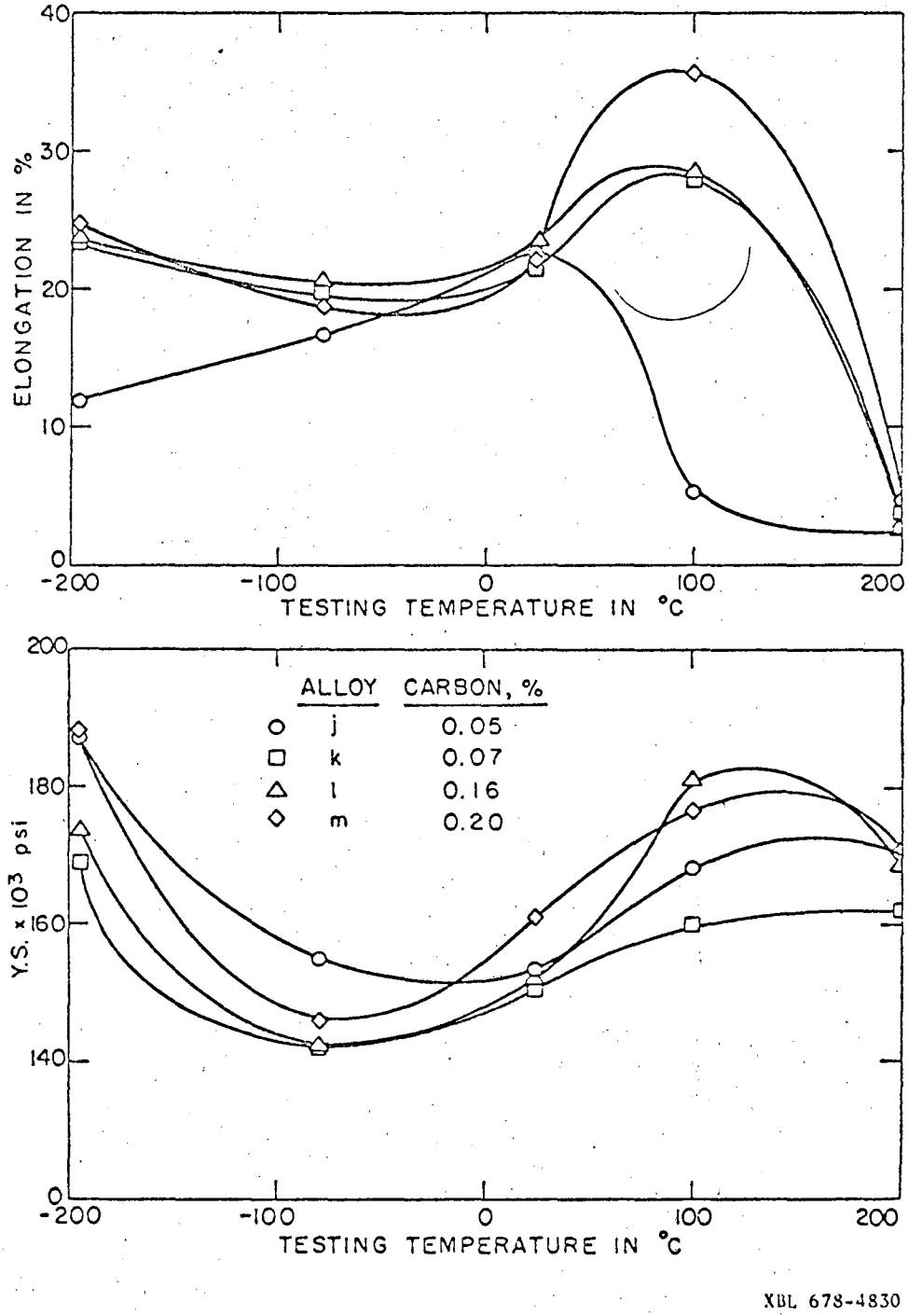
ELONGATION IN %
40
30
20
10
0
-200
-100
0
100
200
TESTING TEMPERATURE IN °C
Y.S. x 10³ psi
200
180
160
140
0
ALLOY CARBON, %
j 0.05
k 0.07
l 0.16
m 0.20
-200
-100
0
100
200
TESTING TEMPERATURE IN °C
XBL 678-4830

Fig. 6

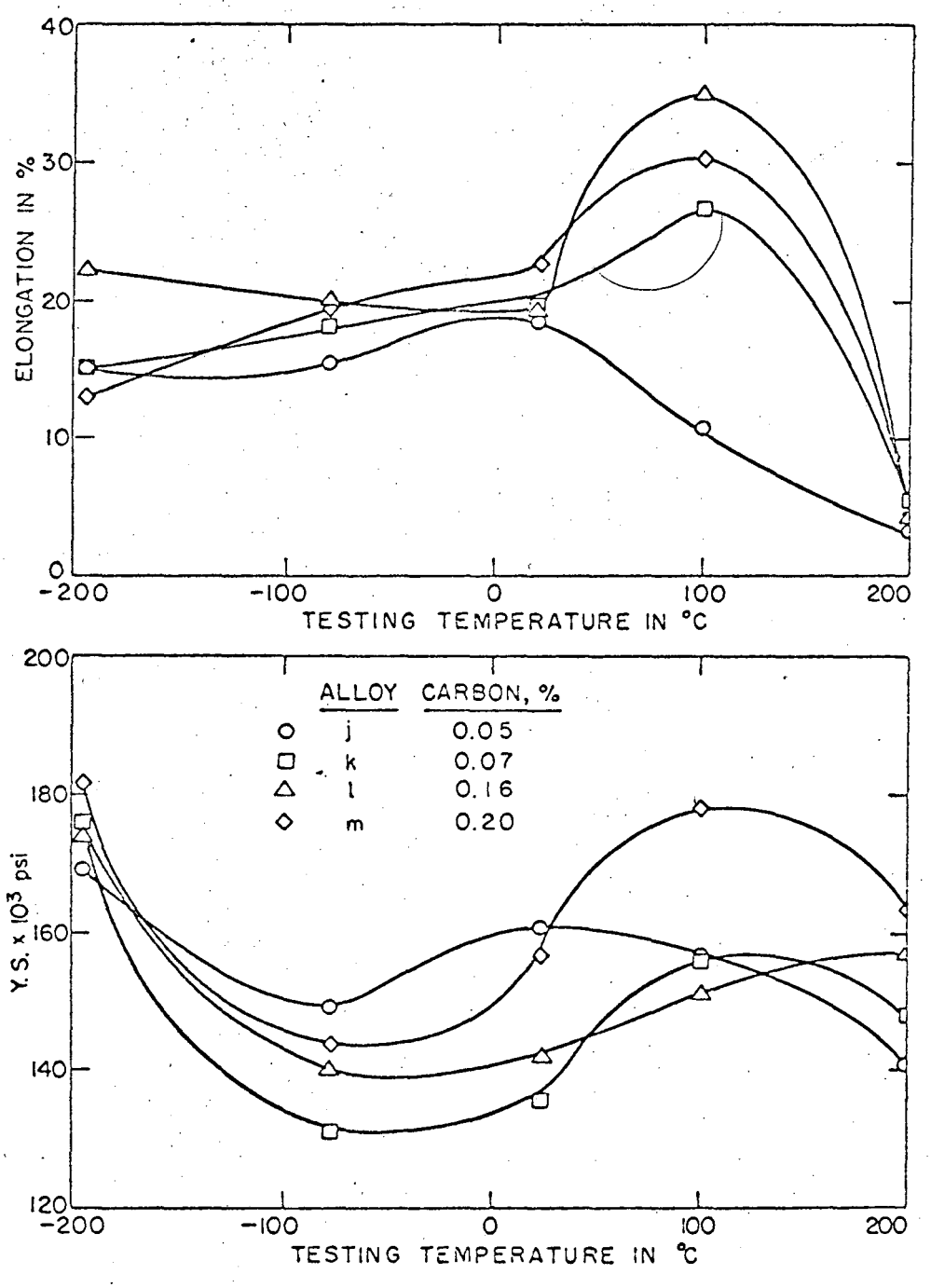
ELONGATION IN %
40
30
20
10
0
-200
-100
0
100
200
TESTING TEMPERATURE IN °C
Y.S. x 10³ psi
200
180
160
140
120
ALLOY CARBON, %
j 0.05
k 0.07
l 0.16
m 0.20
-200
-100
0
100
200
TESTING TEMPERATURE IN °C
XBL 678-4827

Fig. 7

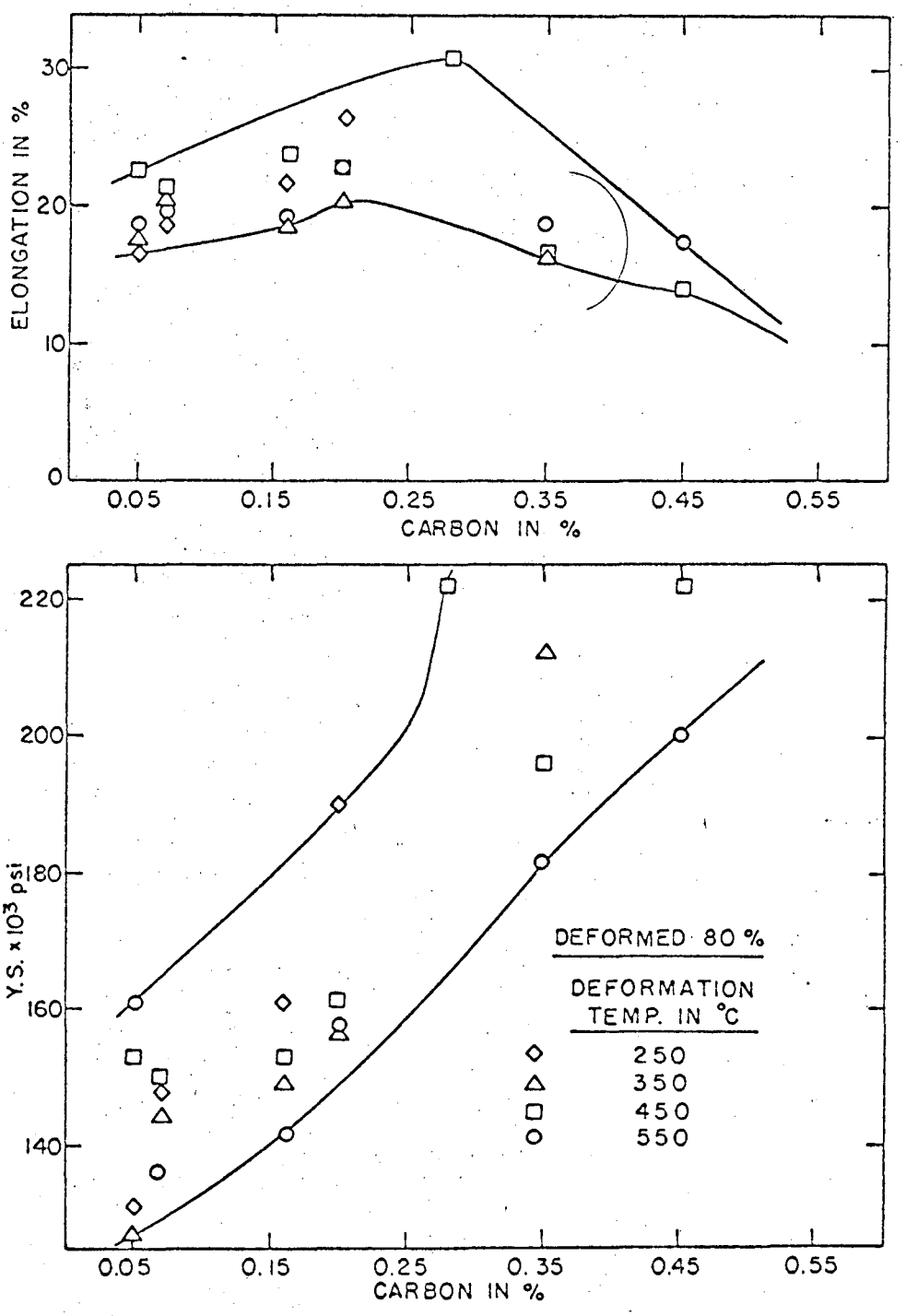

XBL 678-4817

Fig. 8

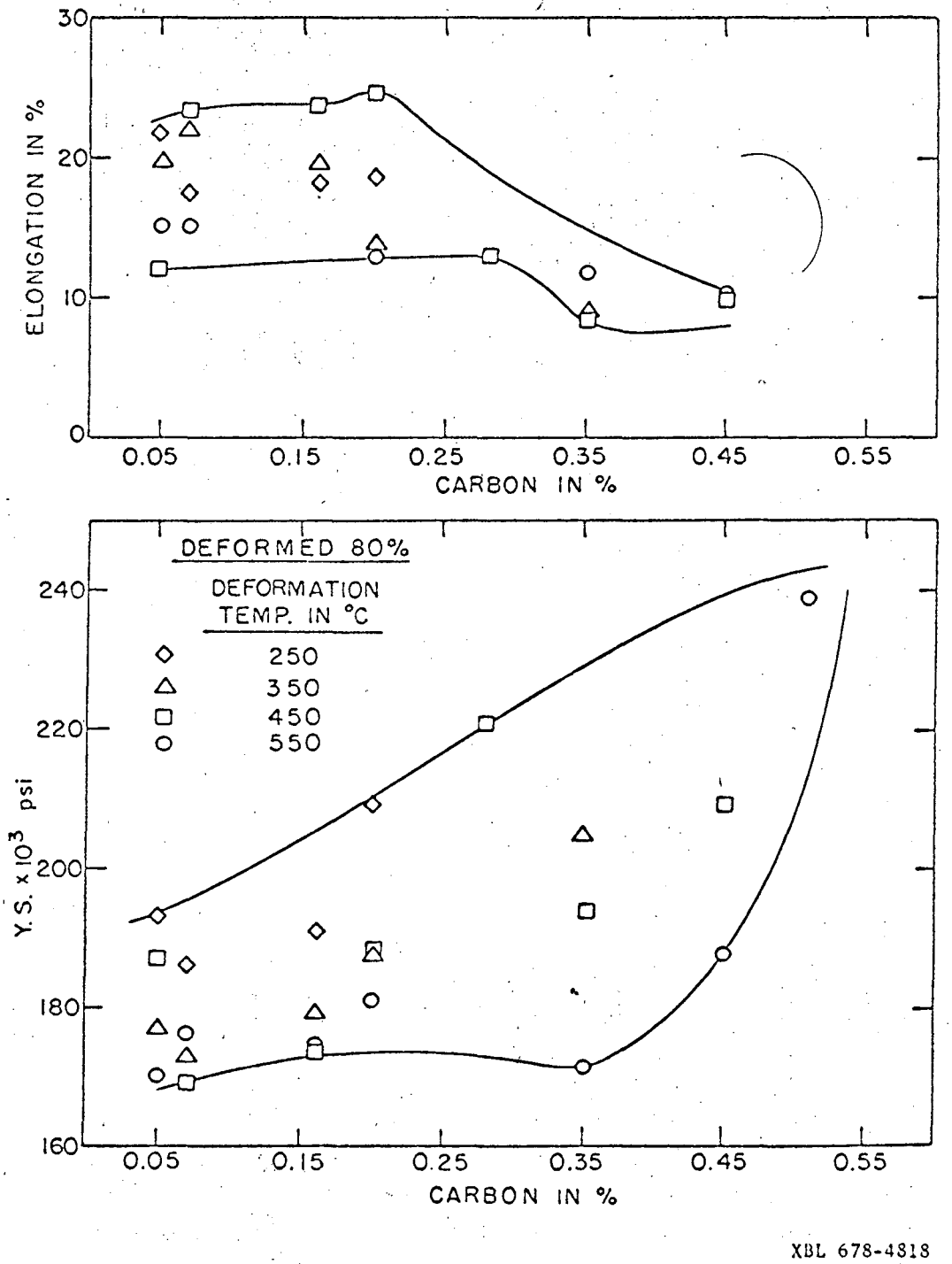
ELONGATION IN %
30
20
10
0
0.05
0.15
0.25
0.35
0.45
0.55
CARBON IN %
DEFORMED 80%
DEFORMATION TEMP. IN °C
250
350
450
550
Y.S. x 10³ psi
240
220
200
180
160
0.05
0.15
0.25
0.35
0.45
0.55
CARBON IN %
XBL 678-4818

Fig. 9

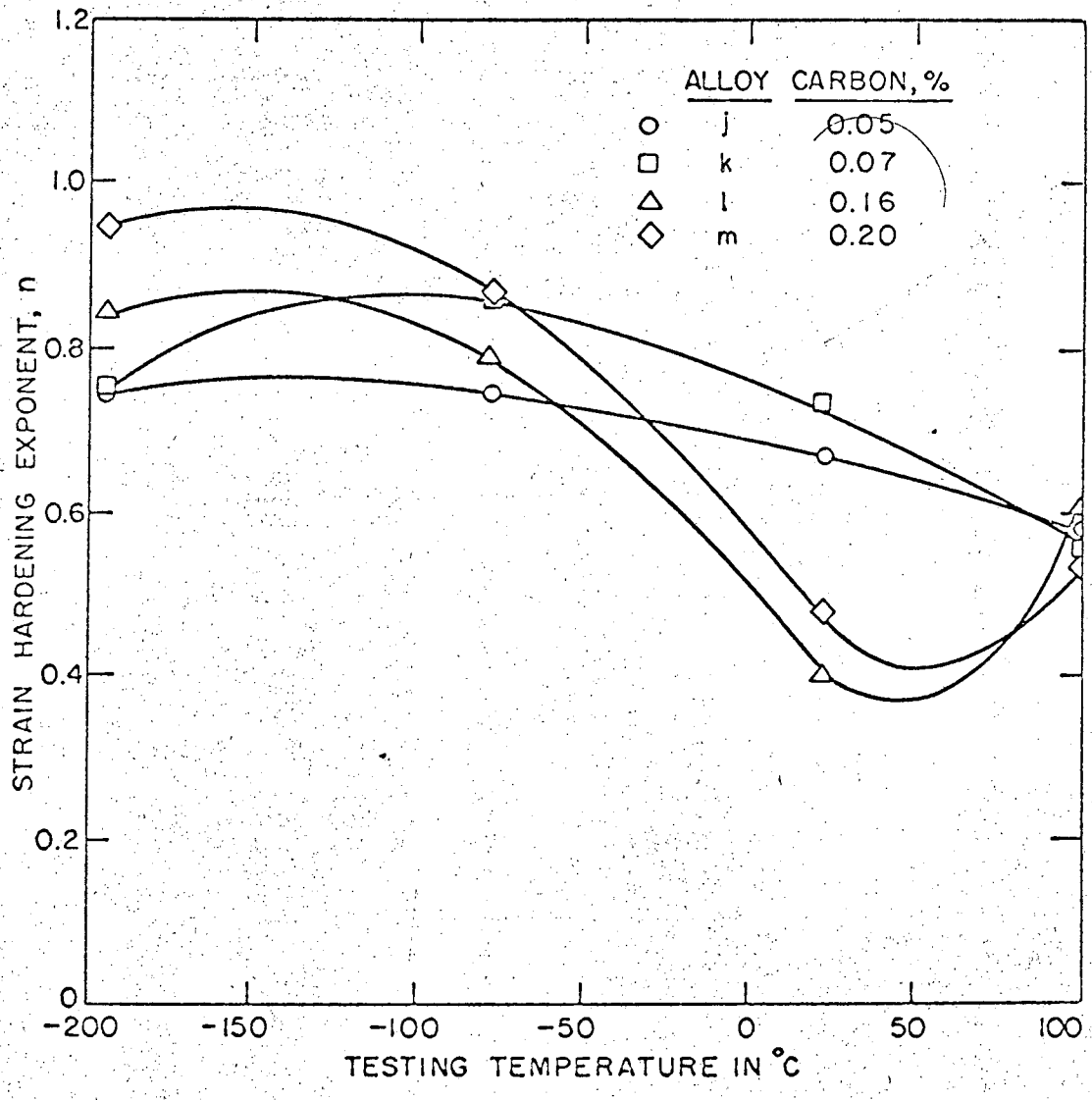

XBL 678-4841

Fig. 10

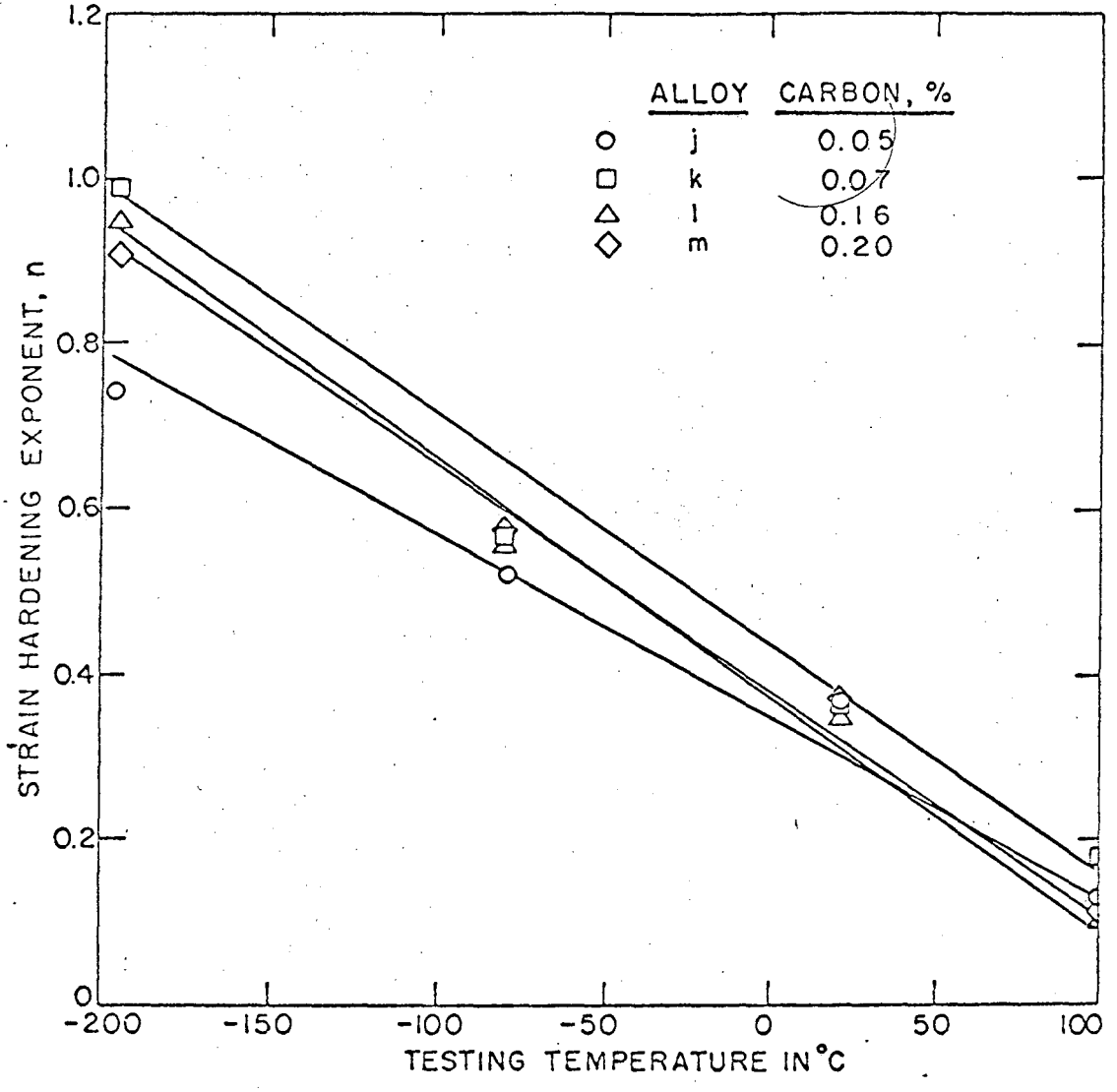

XBL 678-4843

Fig. 11

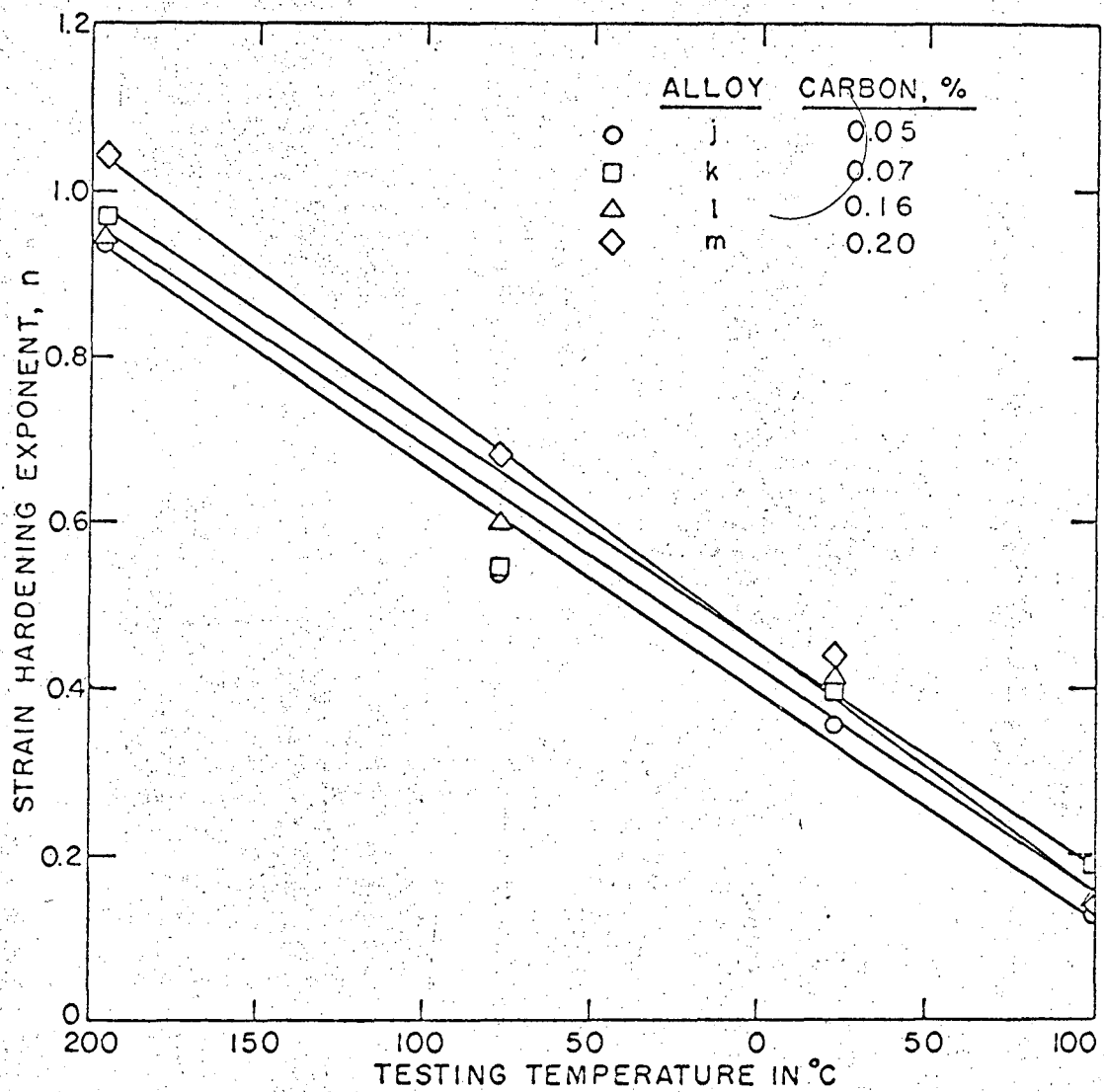

XBL 678-4844

Fig. 12

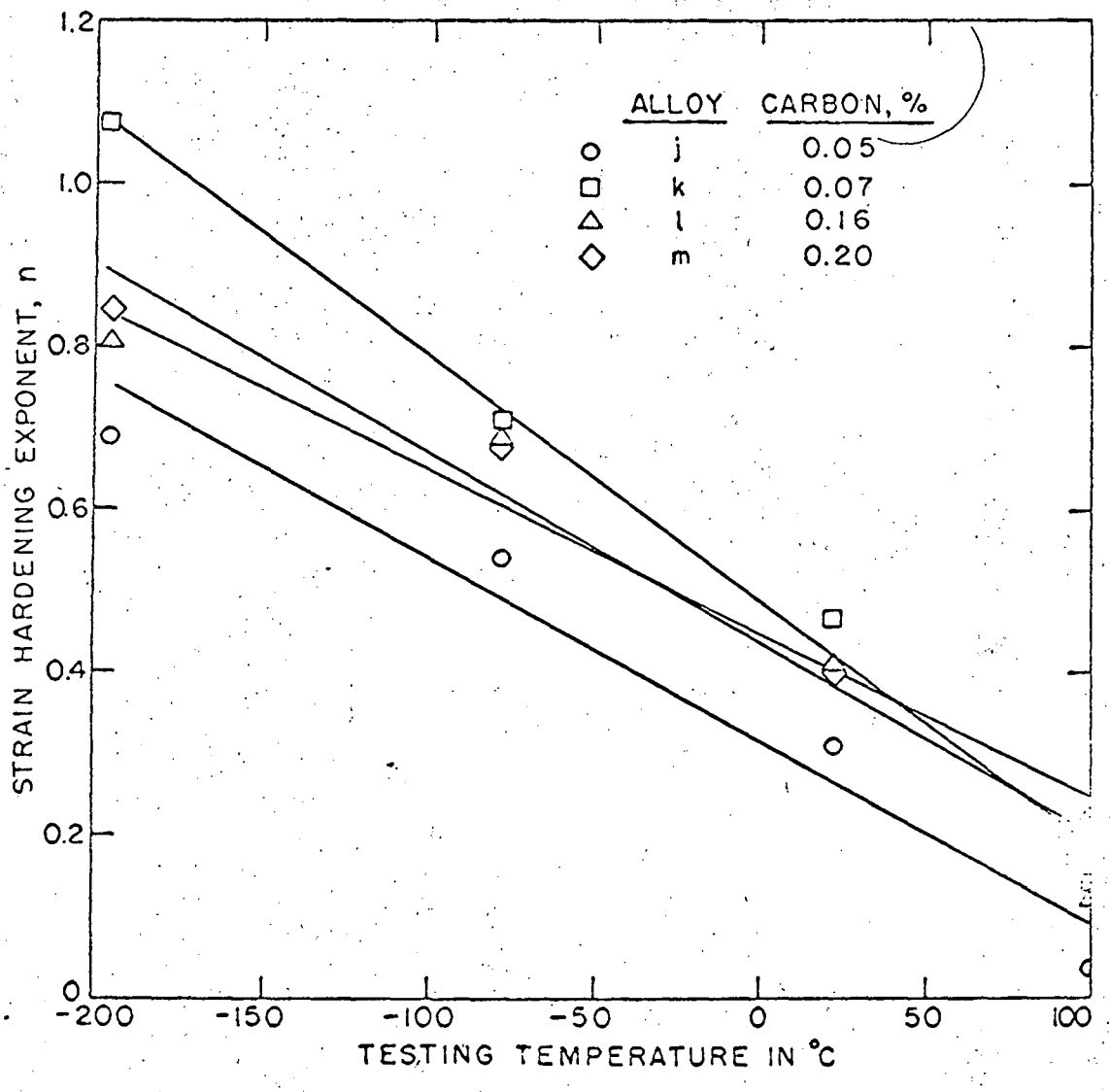

XBL 678-4842

Fig. 13

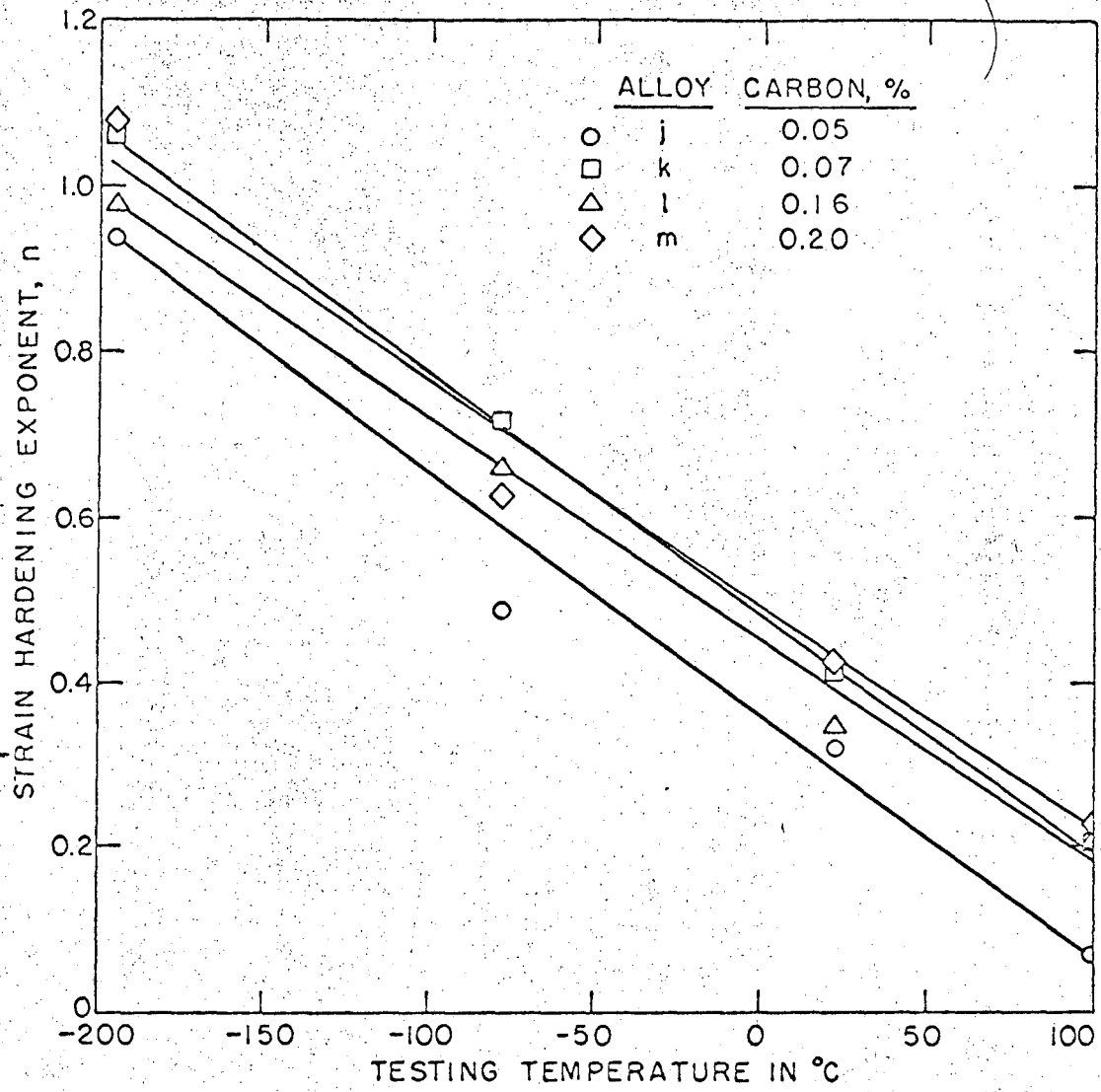

XBL 678-4845

Fig. 14

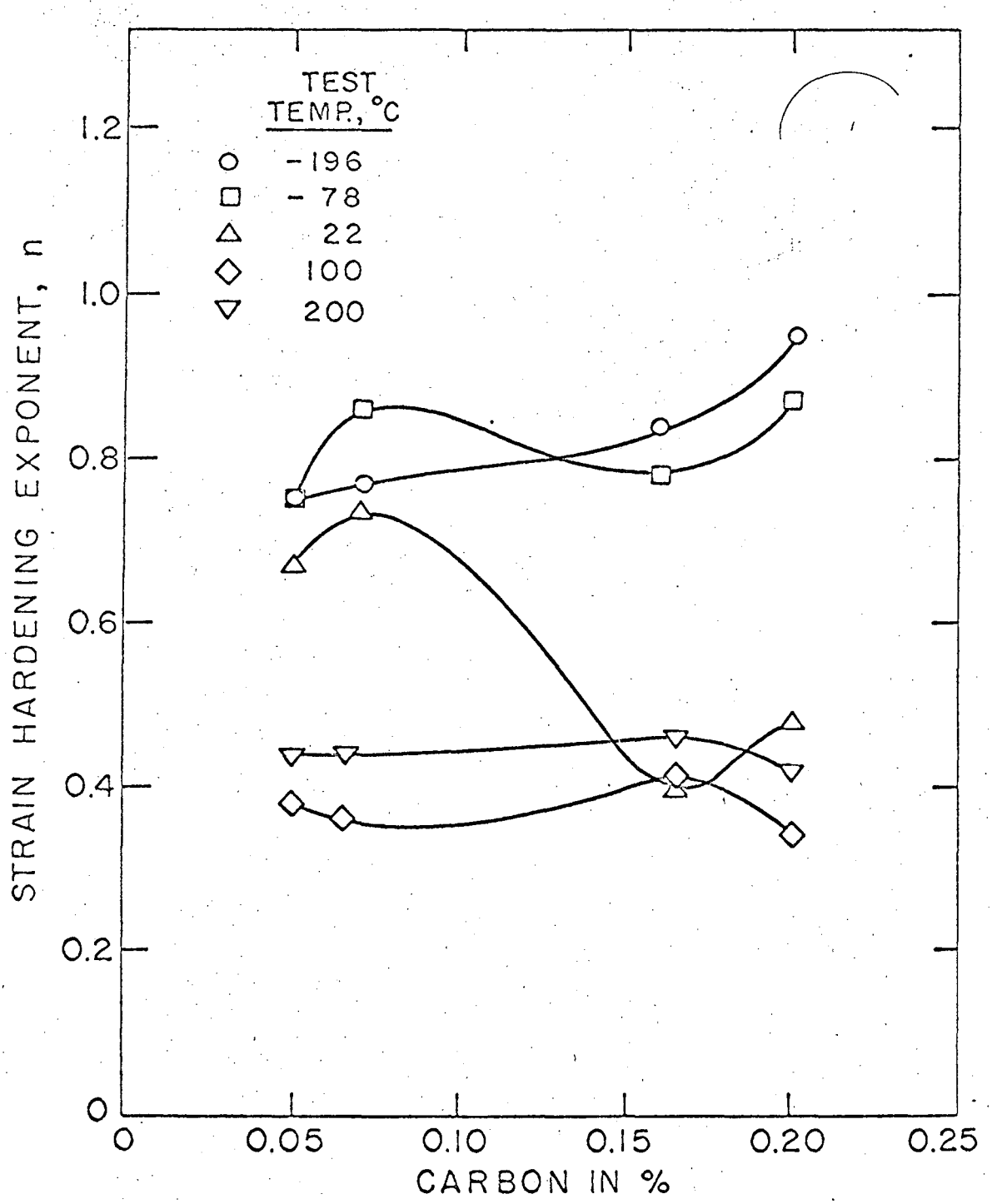

XBL 678-4823

Fig. 15

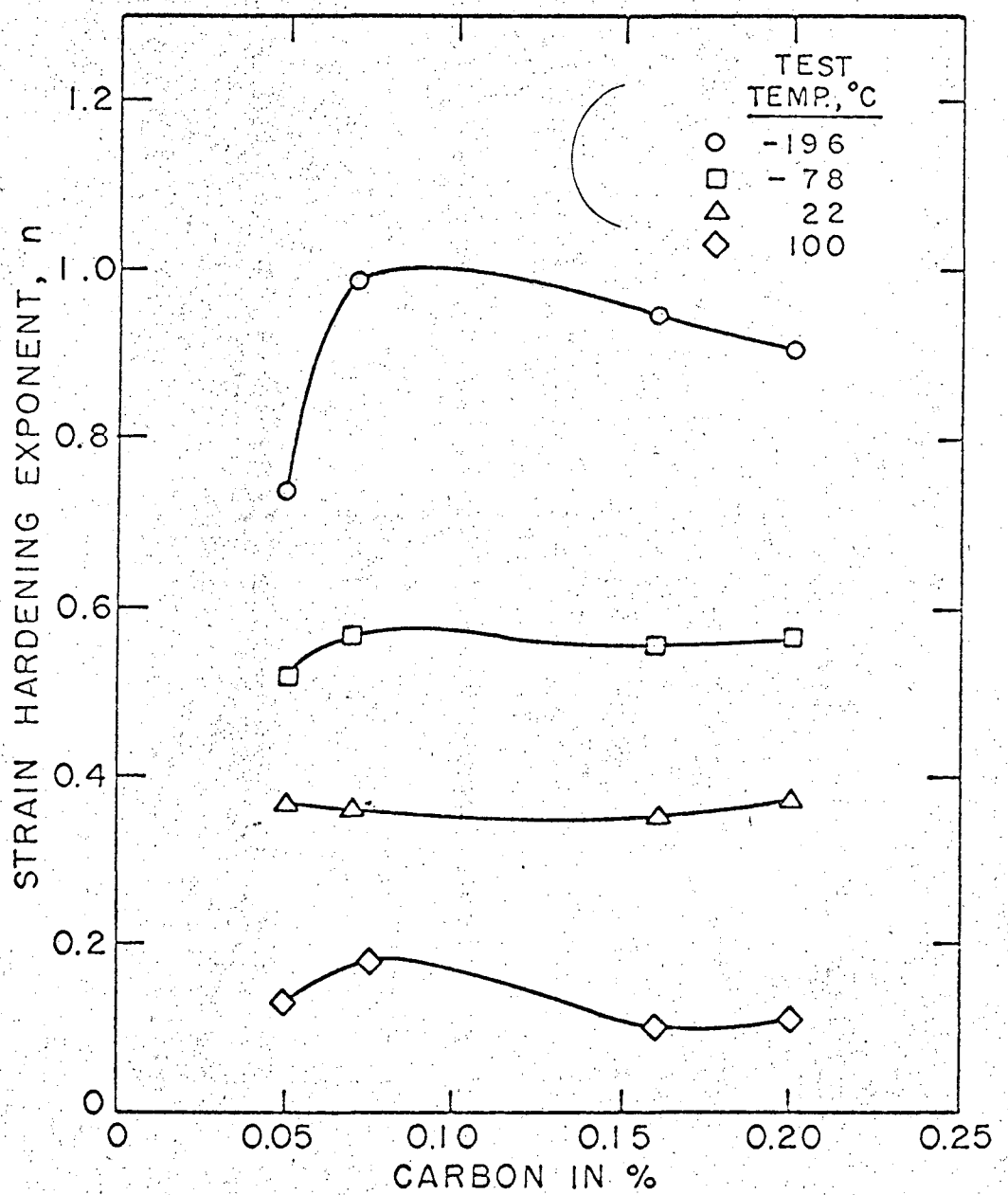
TEST
TEMP., °C
-196
-78
22
100
STRAIN HARDENING EXPONENT, n
1.2
1.0
0.8
0.6
0.4
0.2
0
0
0.05
0.10
0.15
0.20
0.25
CARBON IN %
XBL 678-4822

Fig. 16

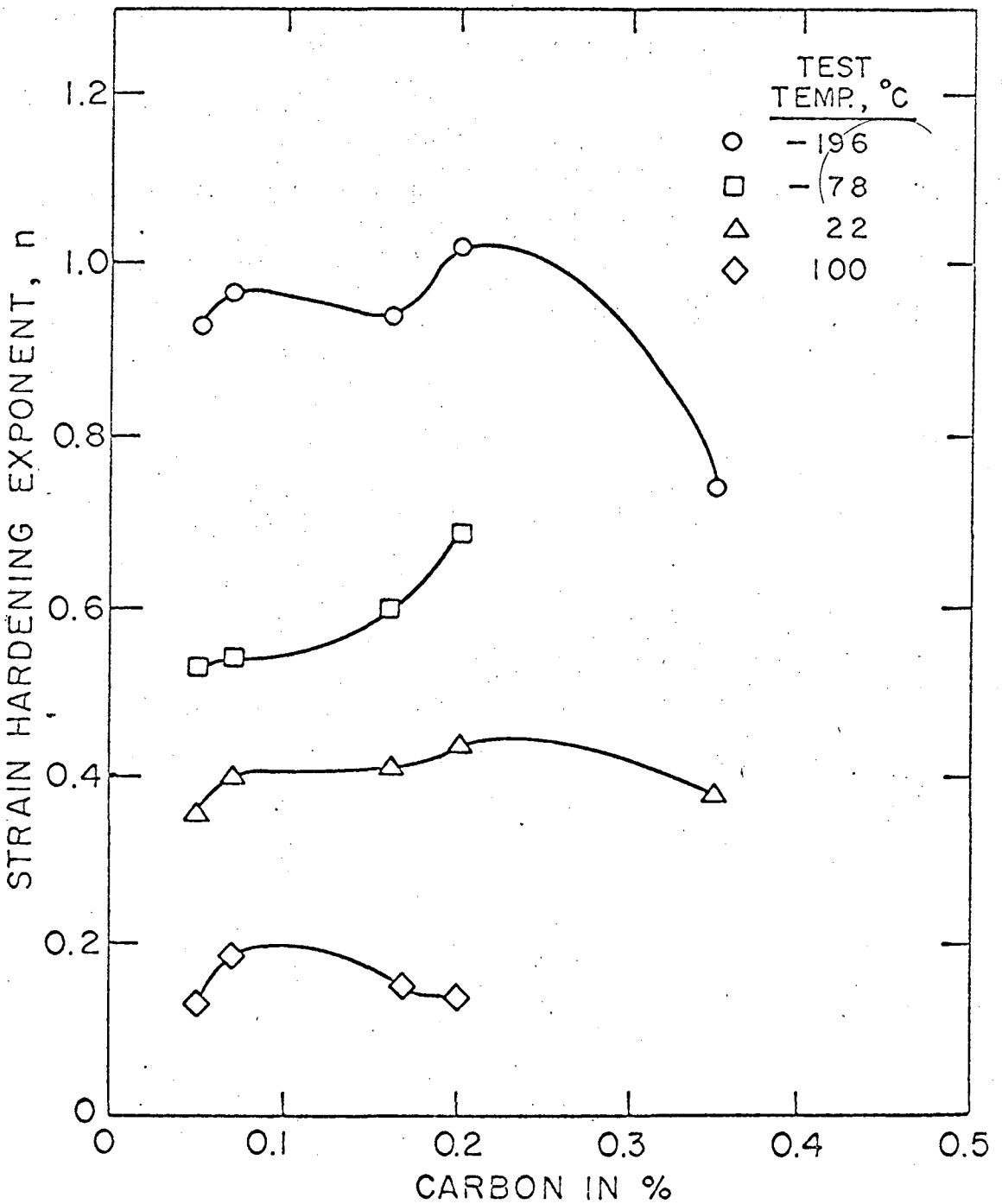

XBL 678-4821

Fig. 17

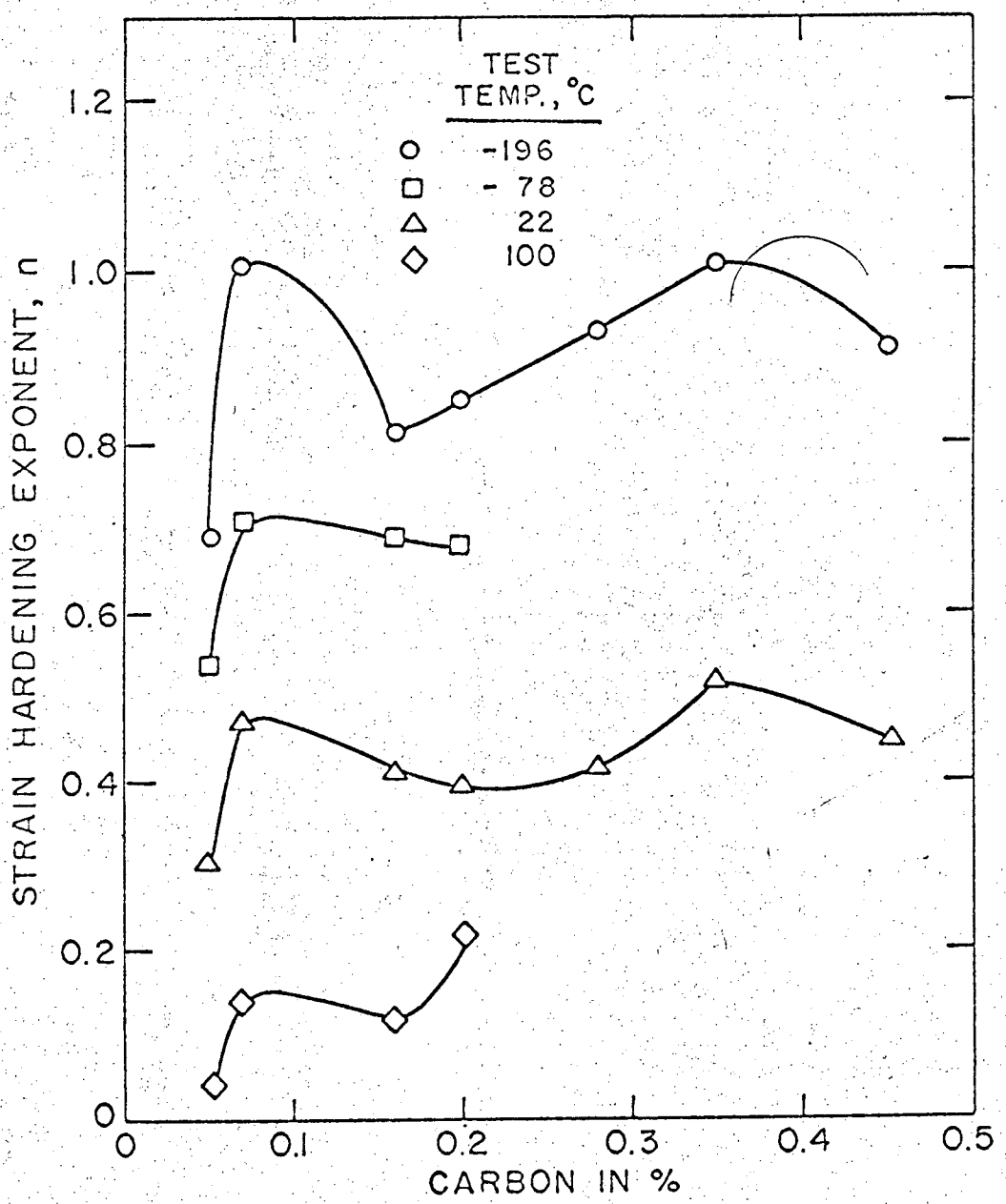

XBL 678-4820

Fig. 18

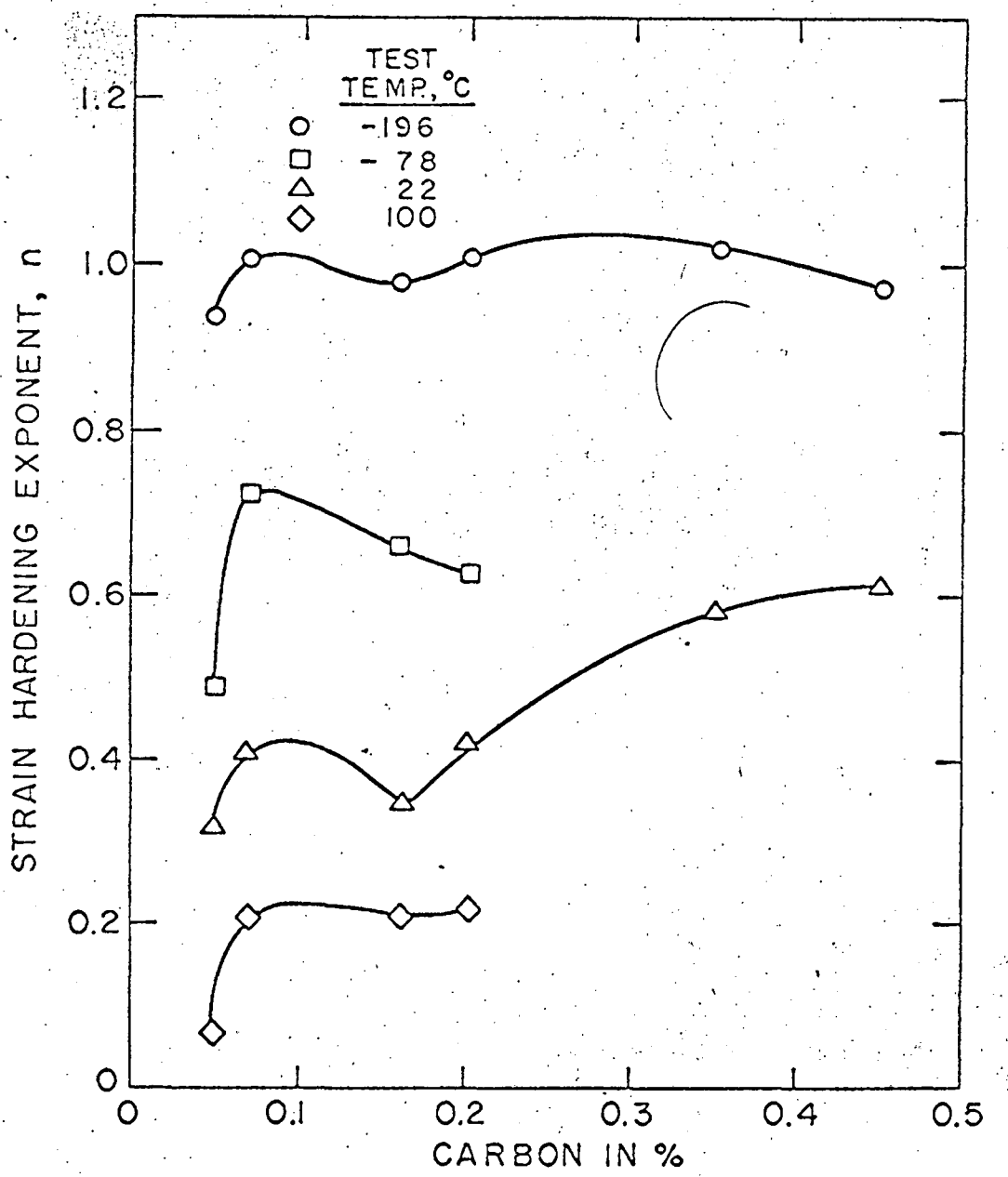

XBL 678-4819

Fig. 19

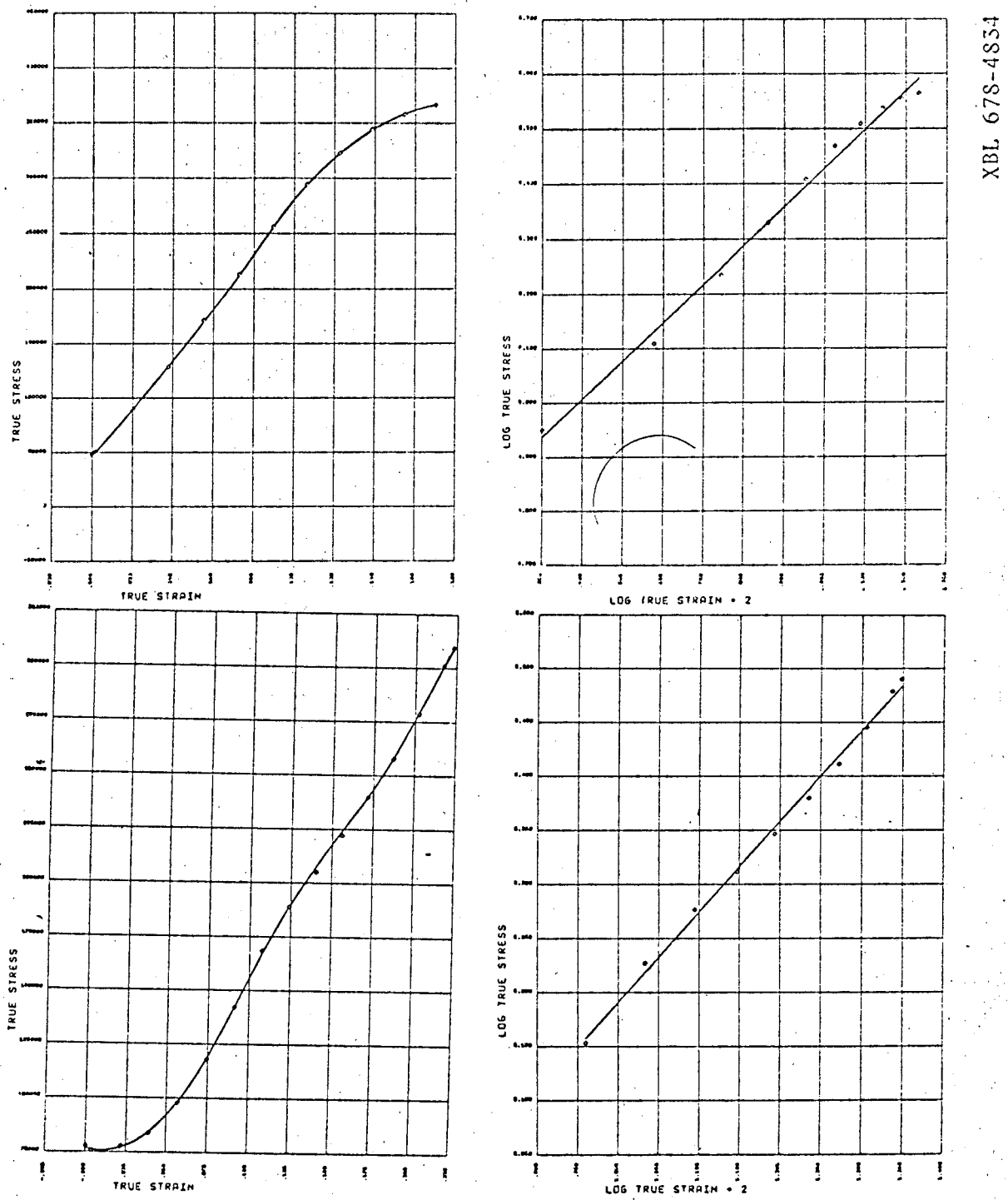

XBL 678-4834

Fig. 20

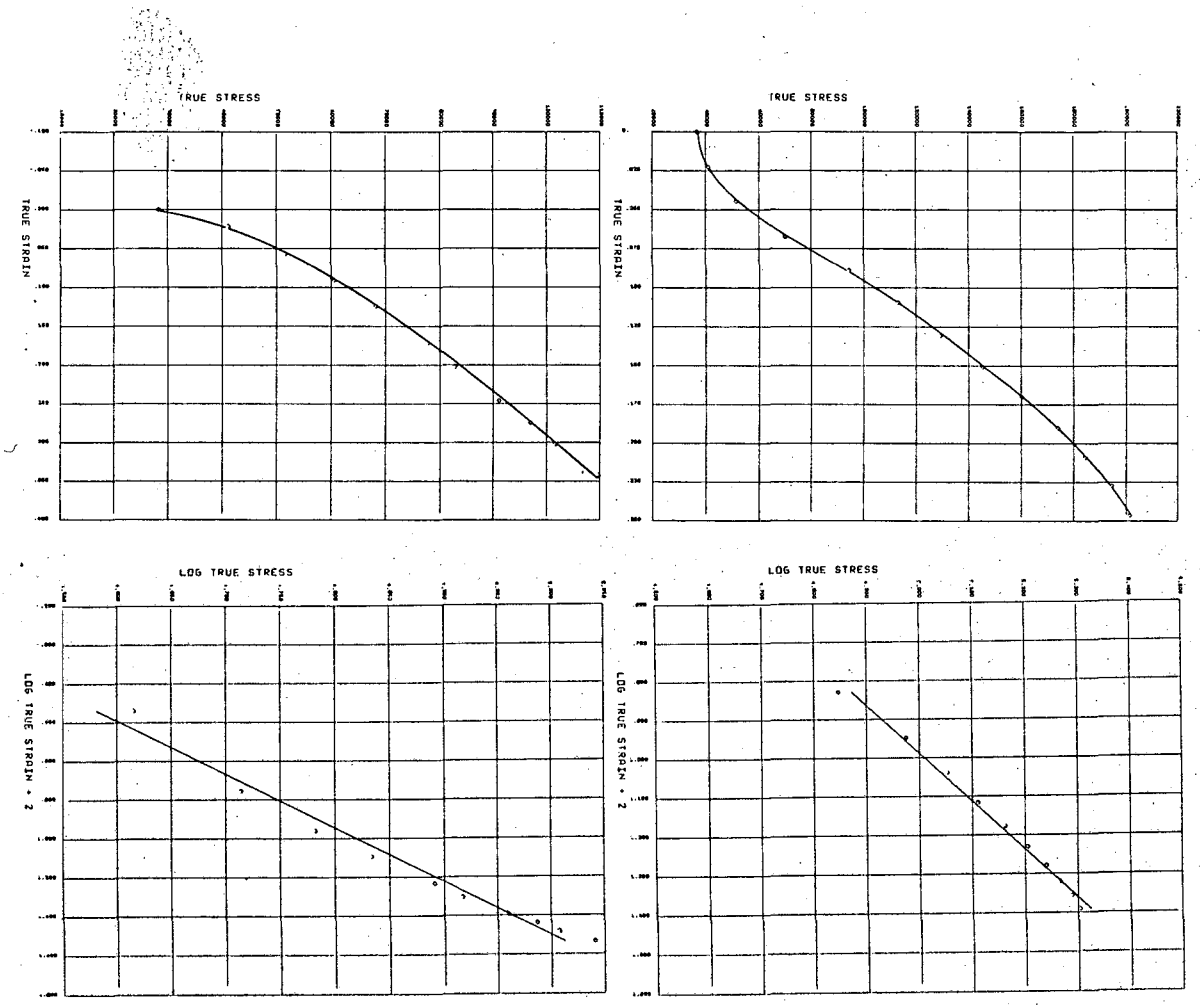

XBL 678-4847

Fig. 21

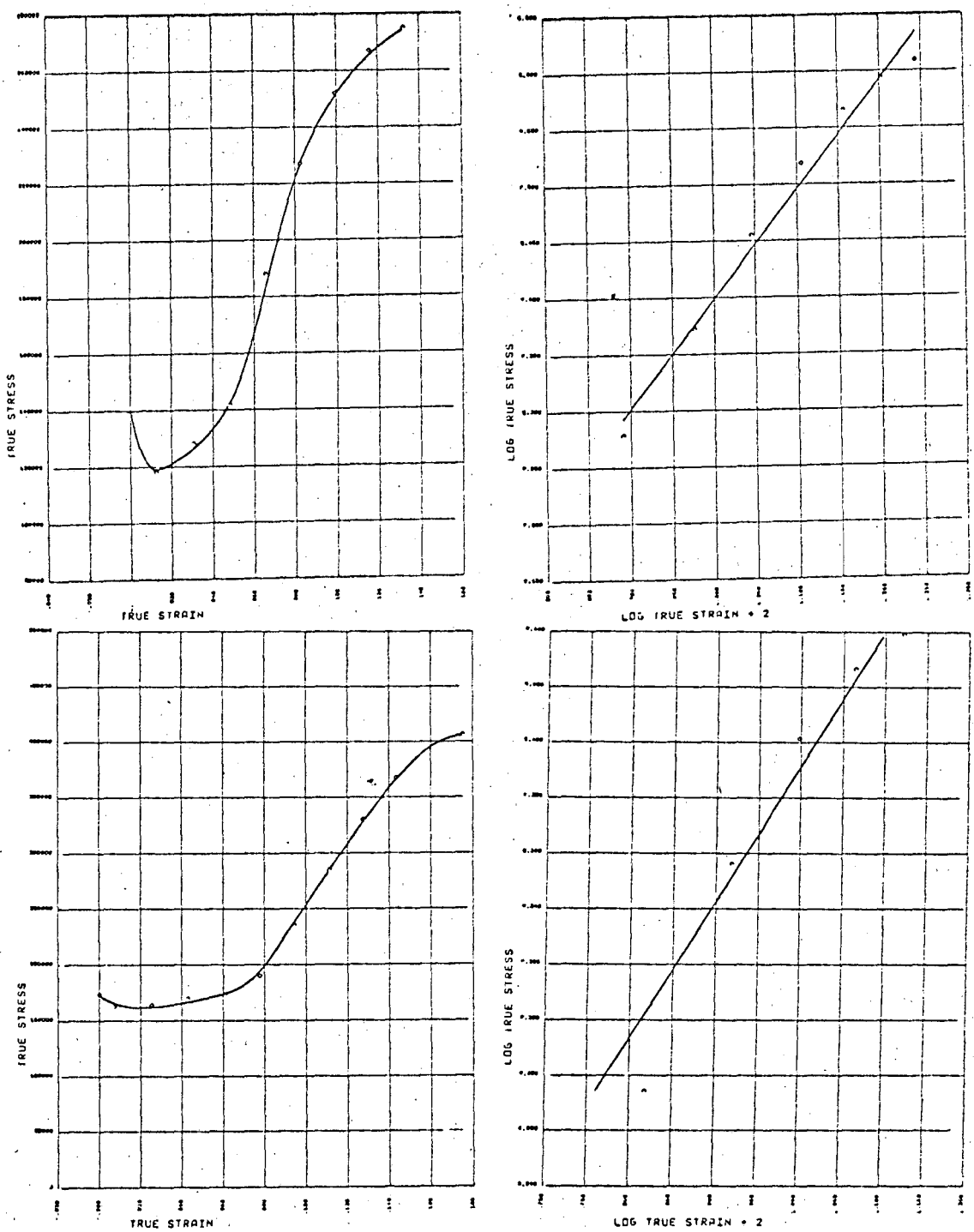

XBL 678-4836

Fig. 22

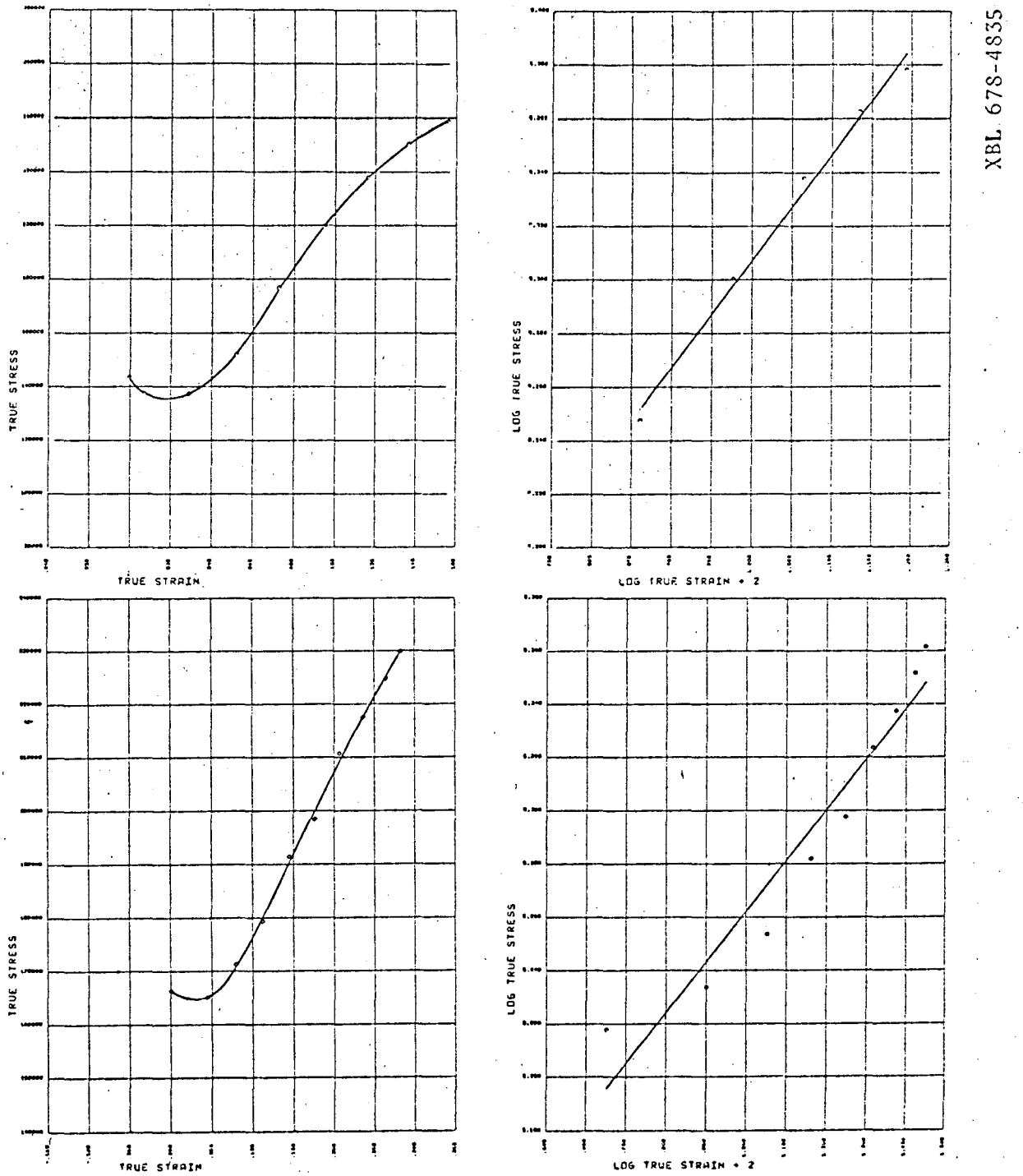

XBL 678-4835

Fig. 23

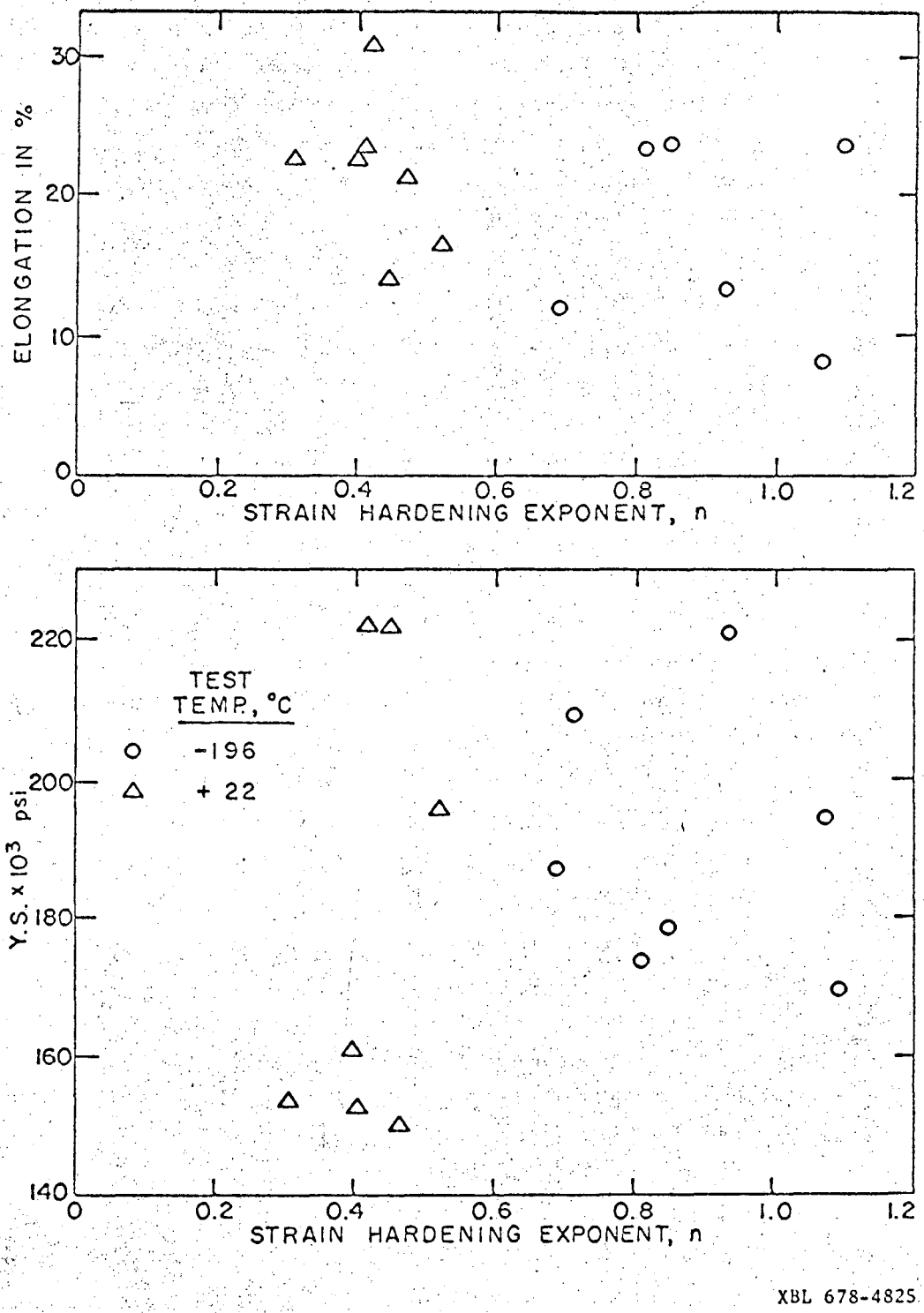
ELONGATION IN %
30
20
10
0
0
0.2
0.4
0.6
0.8
1.0
1.2
STRAIN HARDENING EXPONENT, n
Y.S. x 10³ psi
220
200
180
160
140
TEST TEMP., °C
-196
+ 22
0
0.2
0.4
0.6
0.8
1.0
1.2
STRAIN HARDENING EXPONENT, n
XBL 678-4825

Fig. 24

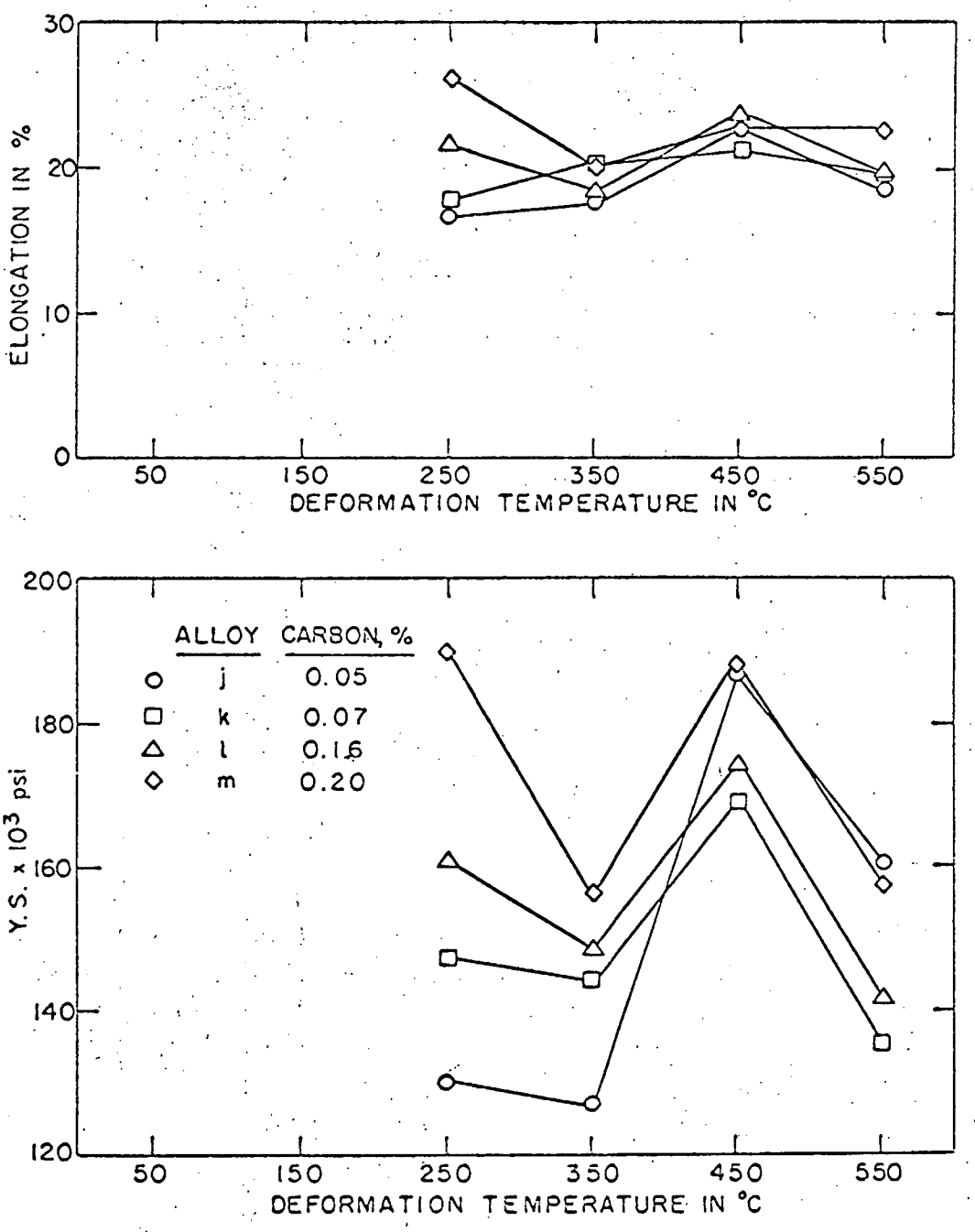
ELONGATION IN %
30
20
10
0
50
150
250
350
450
550
DEFORMATION TEMPERATURE IN °C
Y.S. x 10³ psi
200
180
160
140
120
ALLOY
CARBON, %
j
0.05
k
0.07
l
0.16
m
0.20
50
150
250
350
450
550
DEFORMATION TEMPERATURE IN °C
XBL 678-4824

Fig. 25

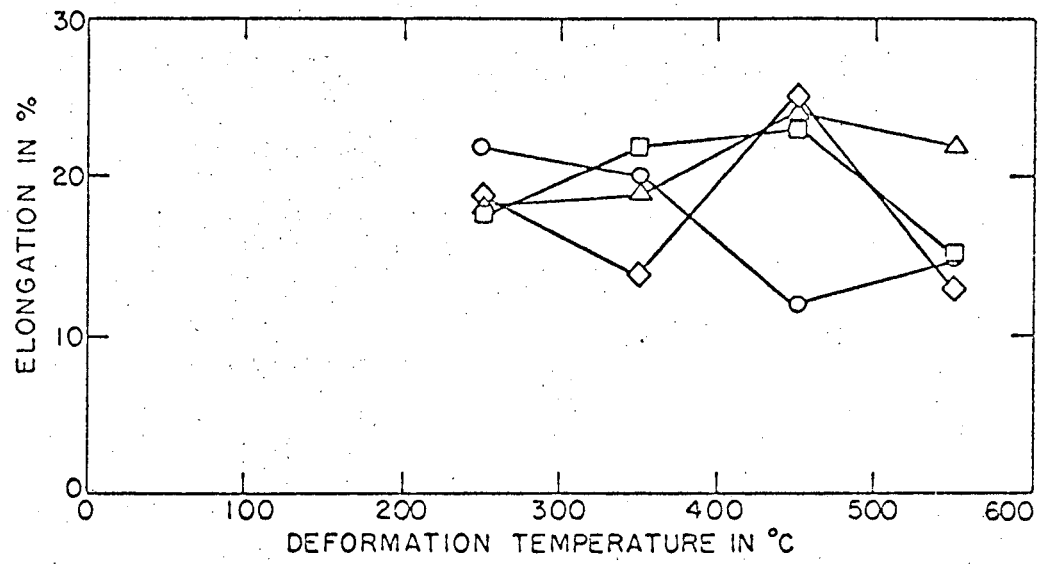

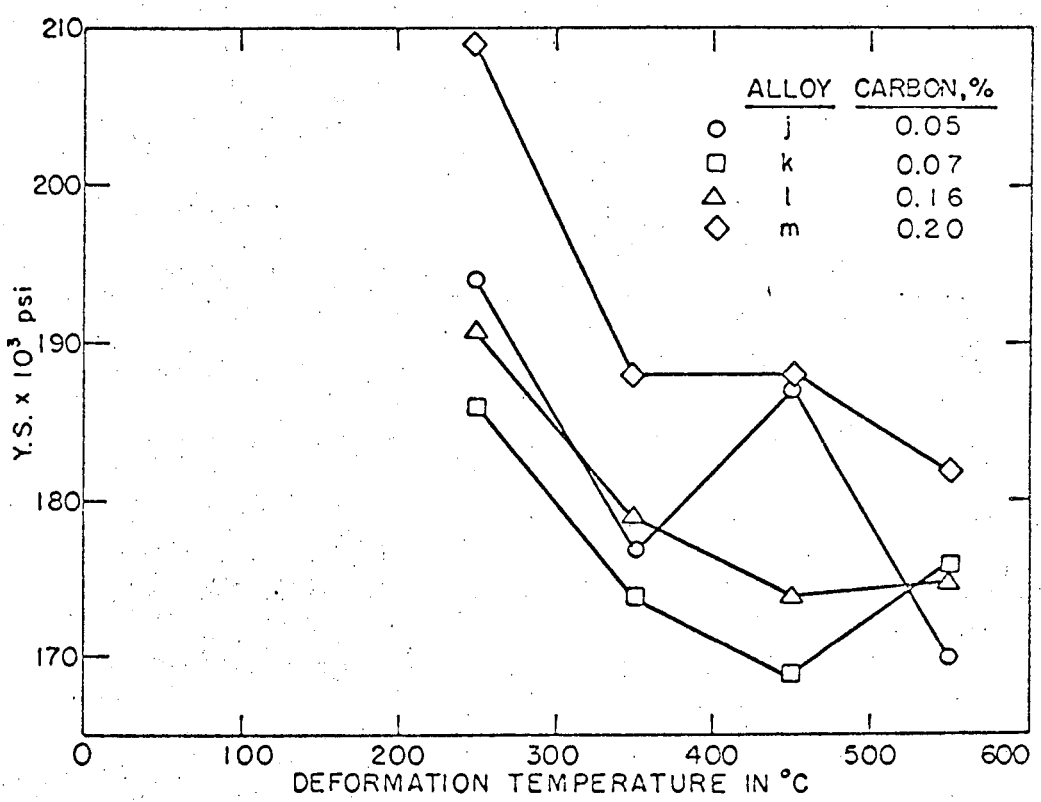

XBL 678-

Fig. 26

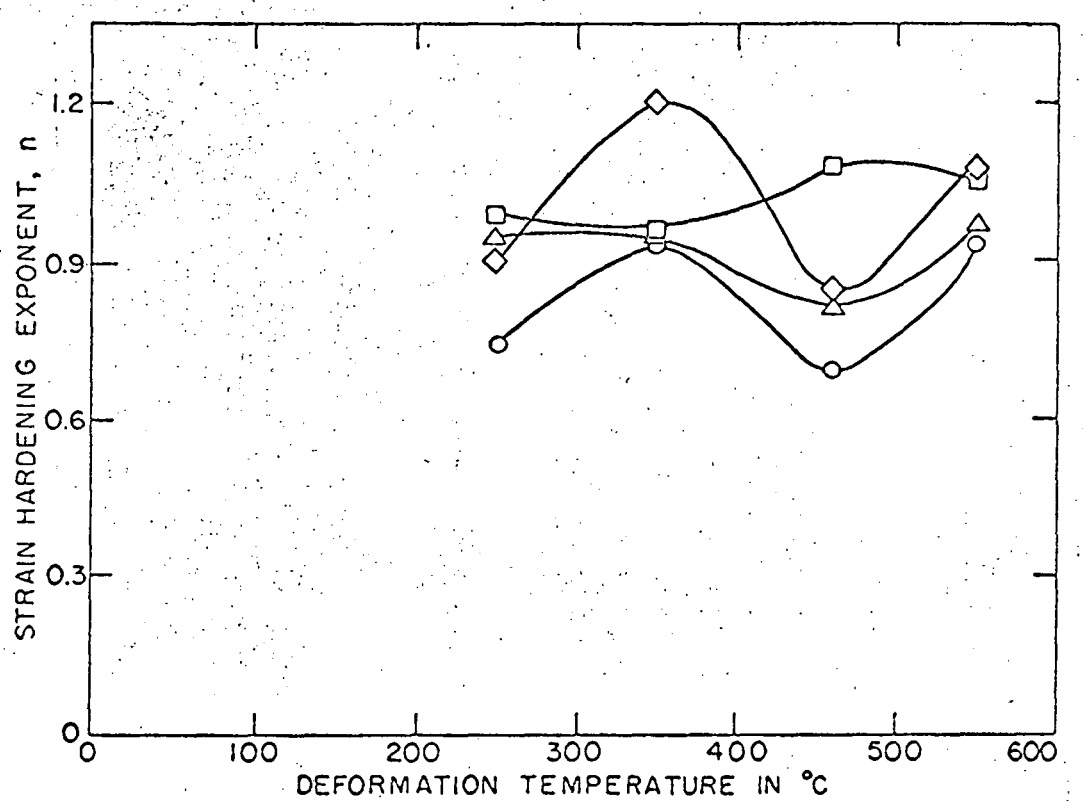

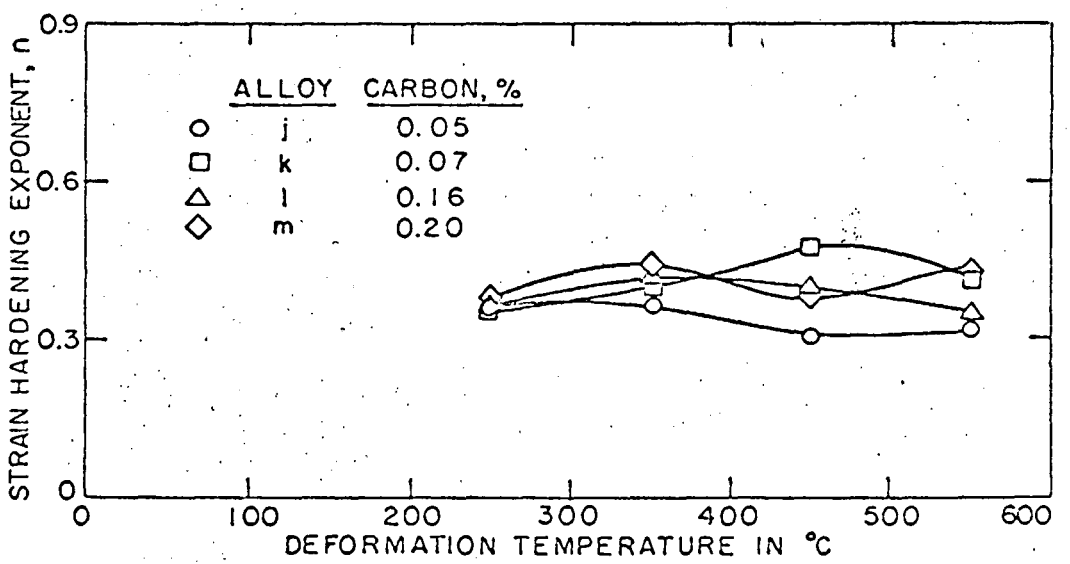

XBL 678-4840

Fig. 27

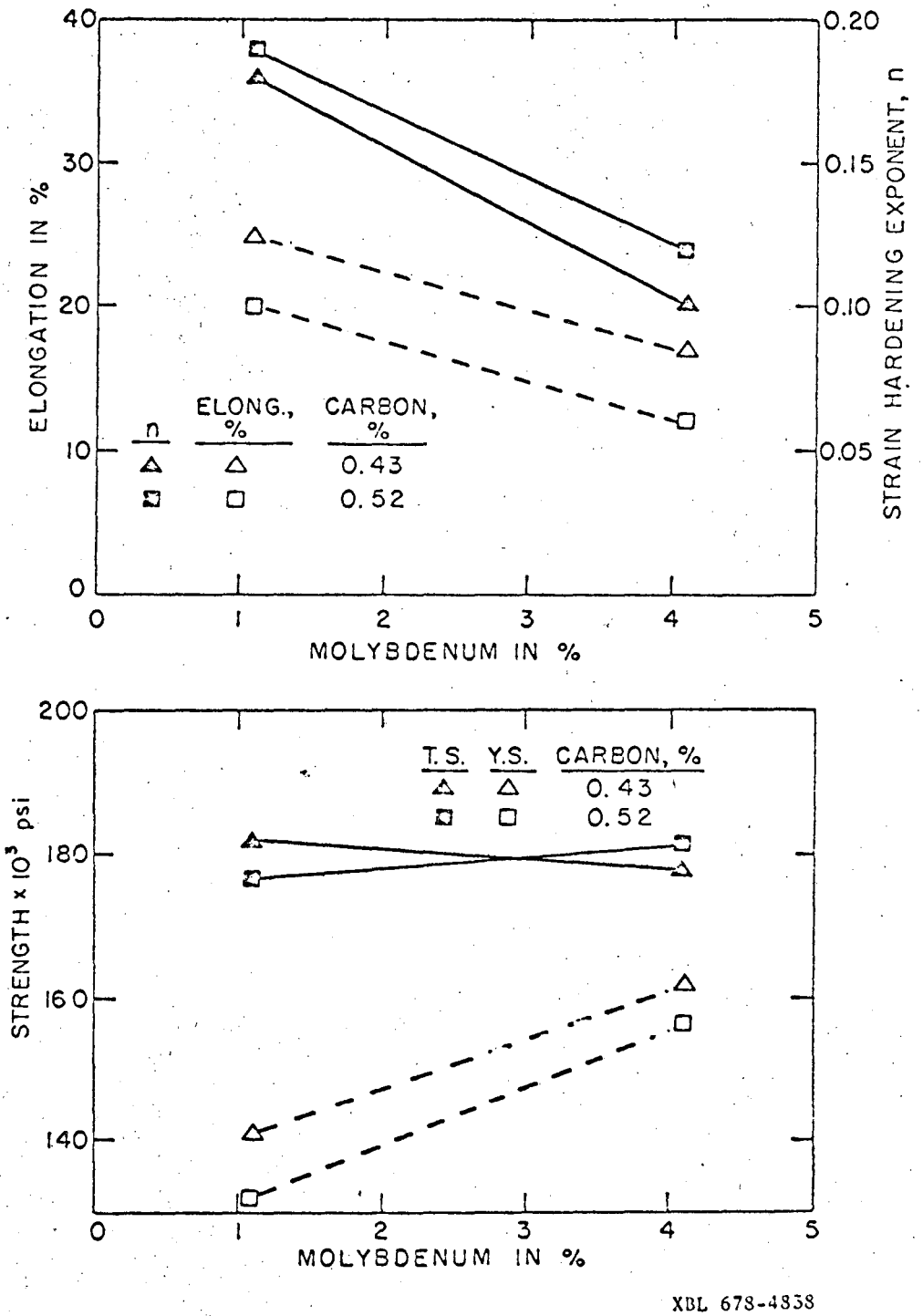
ELONGATION IN %
STRAIN HARDENING EXPONENT, n
MOLYBDENUM IN %
n
ELONG., %
CARBON, %
0.43
0.52
STRENGTH x 10³ psi
T.S.
Y.S.
CARBON, %
0.43
0.52
MOLYBDENUM IN %
XBL 678-4838

Fig. 28

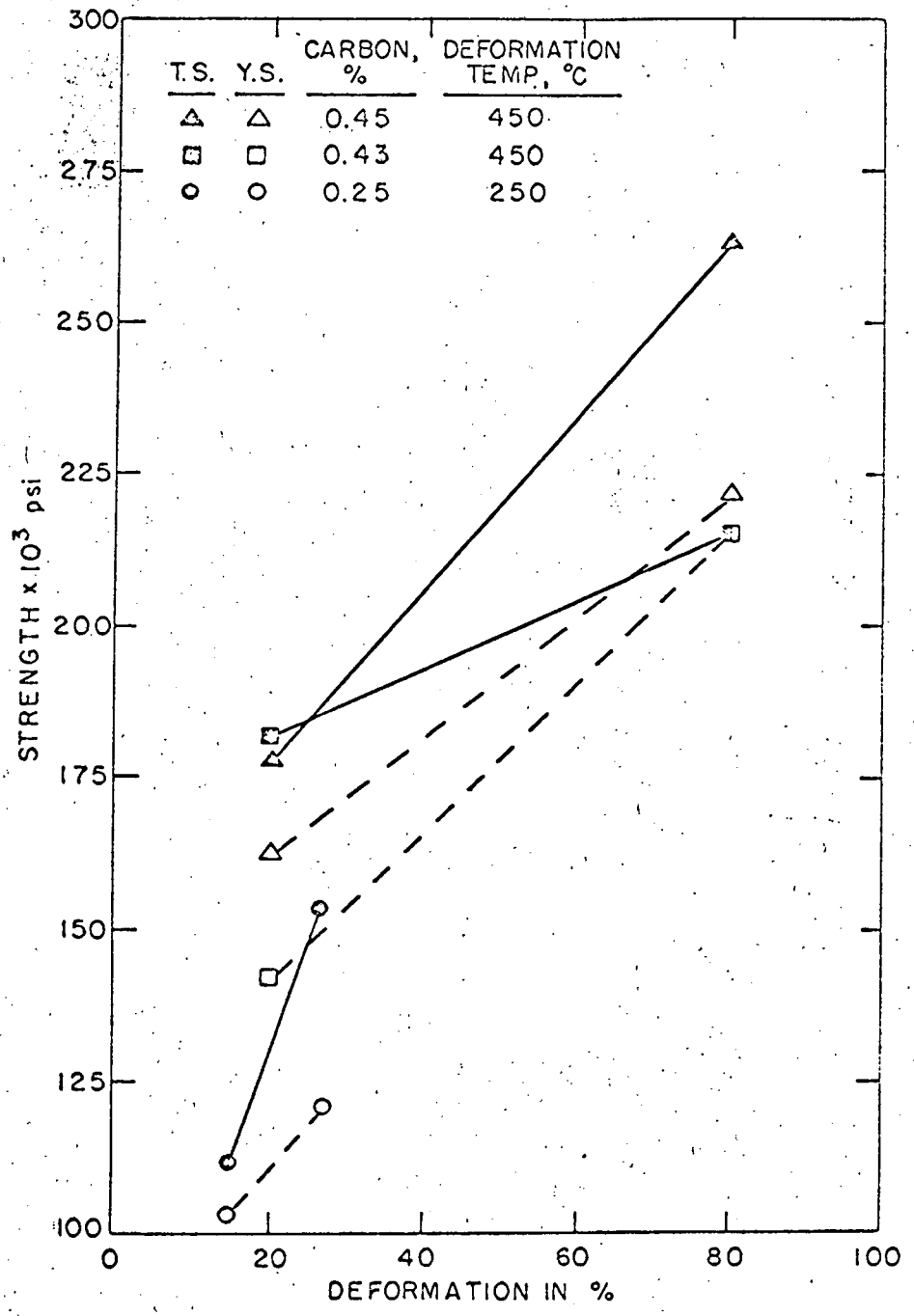

XBL 678-4846

Fig. 29